Soil moisture retrieval from combined Active/Passive Microwave Observations over the Regge and Dinkel

SABAH SABAGHY
February, 2013

SUPERVISORS:
Dr. Ir. Rogier Van der Velde
Dr. Ir. Mhd. Suhyb Salama

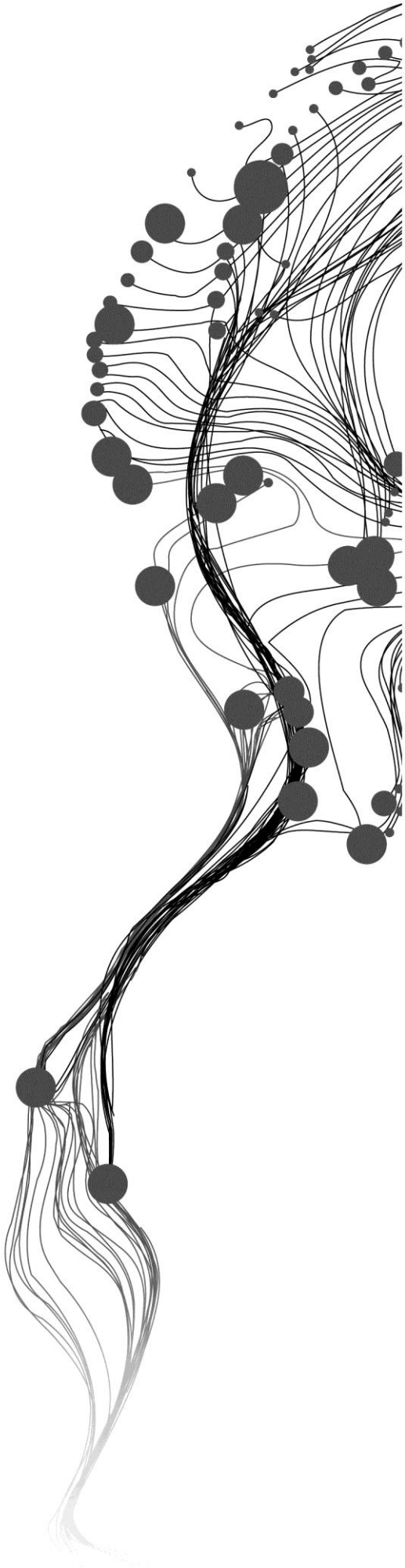

Soil moisture retrieval from combined Active/Passive Microwave Observations over the Regge and Dinkel

SABAH SABAGHY
Enschede, the Netherlands, February, 2013

Thesis submitted to the Faculty of Geo-Information Science and Earth Observation of the University of Twente in partial fulfilment of the requirements for the degree of Master of Science in Geo-information Science and Earth Observation.
Specialization: Water Resources and Environmental Management (WREM)

SUPERVISORS:
Dr. ir. R. (Rogier) Van der Velde
Dr. ir. M.S. (Suhyb) Salama

THESIS ASSESSMENT BOARD:
Prof. dr. ing. W. (Wouter) Verhoef (Chair)
Dr. S. Monincx (External Examiner, Water Board of Regge and Dinkle)

ABSTRACT

Monitoring soil moisture as a hydrological variable is vital for quantifying the exchange of water, energy and carbon fluxes between land and atmosphere. Several studies have shown that combining active and passive microwave observations is a promising technique to retrieve accurate soil moisture at higher resolution. The proposed algorithm for the future NASA's Soil Moisture Active/Passive (SMAP) mission is the recent change detection approach providing absolute soil moisture contents. This algorithm, hereafter referred to as the SMAP algorithm, is based on the near linear relationship between volumetric soil moisture and radar backscatter.

We adopt the SMAP algorithm for retrieving soil moisture and apply it to the passive (VUA-NASA AMSR-E) soil moisture products and corresponding active (PALSAR ScanSAR) backscatter data set acquired over the eastern part of the Netherlands in 2008 and 2010. Through this process, soil moisture contents are produced at two medium resolutions equal to 1-km and 5-km. Both soil moisture retrievals are compared against in-situ measurements in Twente region. Obtained RMSE's from this comparison are on average 0.068 and 0.058 m^3m^{-3} for retrievals at 1-km and 5-km, respectively. These results demonstrate the potential of the SMAP algorithm in monitoring reasonably accurate soil moisture products with fair representation of the regional soil moisture. Application of the SMAP algorithm at different medium resolutions also results in obtaining different information on the temporal and spatial variability of soil moisture.

Keywords: soil moisture, combined Active/Passive microwave, SMAP, PALSAR ScanSAR, AMSR-E, L-band backscatter response.

ACKNOWLEDGEMENTS

I would like to express my heartfelt appreciation to my supervisors for their invaluable guidance and encouragement throughout the thesis period. My sincere gratitude goes to my primary supervisor Dr. Rogier Van der Velde who introduced this wonderful research topic to me. Rogier's supervision, critical criticism and advice enabled me to reach a strong background of the subject. He has always had confidence in me and my work which stimulated me to work harder at every stage of this research. Secondly, I am grateful to my second supervisor Dr. Suhyb Salama for his motivation. The discussions I had with him gave me real insight into the study.

I would like to thank the EU Erasmus Mundus LOT8- scholarship scheme for funding my studies. It has been a great opportunity to improve my skills, experience and qualifications on this course and I feel greatly indebted. Further, I acknowledge the European Space Agency (ESA) for granting the PALSAR data set. To all my friends that made this study period an amazing multicultural experience, I would like to say a big thank you. You all were there for me through the thick-and-thin of our stay in the Netherlands and I am lucky to have met each one of you.

Dear Uncle Dimitri and Aunt Yoke, I would like to thank you for your support during my stay in the Netherlands. With your great love I did not feel lonely at all. Thank you for treating and protecting me like your own daughter.

My lovely parents are sincerely acknowledged for giving me the strength and confidence to pursue my vision. You are indeed my inspiration. My siblings also deserve my deepest gratitude. My sister, Layla, always cheered me up when I felt tired and stressed. Then, there was my brother, Hamed, who kept me standing by telling me to, "Aim for the best, you have the potential". What would I have done without you, my family!

List of Abbreviations

AIRSAR……...Airborne SAR
ALOS…….…….Advance Land Observing Satellite
AMSR-E……Advanced Microwave Scanning Radiometer for Earth observation system
ASAR……...Advanced SAR
EASE-Grid……..…...Equal-Area Scalable Earth Grid
EOS……...……Earth Observing System
ERS……European Remote Sensing
ESA……European Space Agency
GCPs……...Ground Control Points
HDF-EOS……...Hierarchical Data Format- Earth Observing System
Hydros…… Hydrosphere state
IR……Infrared
JERS……...Japanese Earth Resources Satellite
IDL..……. ……Interface Description Language
LPRM……Land Parameter Retrieval Model
MAE……...Mean Absolute Error
MIRAS…….Microwave Imaging Radiometer with Aperture Synthetic
MODAGG…….MODIS surface reflectance AGGregation
MODIS……...MODerate resolution Imaging Spectrometer
NASA……National Aeronautics and Space Administration
NDVI……...Normalized Difference Vegetation Index
NEST……Next ESA SAR Toolbox
OSSE……...Observation System Simulation Experiment
PALS……Passive/Active L-band System
PALSAR……Phased Array L-band SAR
RFI……Radio Frequency Interference
RMSE……Root Mean Square Error
SAR……...Synthetic Aperture Radar
SCI…….Single Channel I
ScanSAR……Scanning SAR
SGP99……...1999 Southern Great Plains
SMAP……Soil Moisture Active and Passive
SMEX02……..Soil Moisture Experiment 2002
SMOS……Soil Moisture and Ocean Salinity
VI……..Vegetation Index
VIS……Visible
VUA……Vrij Universiteit Amsterdam

TABLE OF CONTENTS

LIST OF FIGURES

LIST OF TABLES

1. INTRODUCTION

1.1. Scientific Background

Soil moisture as a land state variable plays an important role in the various components of the water and energy cycle such as evapotranspiration, deep drainage and surface runoff. Consequently, soil moisture monitoring is vital for quantifying the exchange of water, energy and carbon fluxes between land and atmosphere. Microwave remote sensing has the potential of augmenting sparsely distributed measurements of soil moisture from in-situ networks (Njoku et al., 2002). Microwave observations have the advantage of being able to penetrate clouds (Njoku & Entekhabi, 1996) allowing a continuous monitoring of the land surface.

Although L-band passive microwave measurements are considered to be the most appropriate technique for soil moisture mapping (i.e. Calvet et al., 2011; Njoku et al., 2002; Schmugge et al., 2002) in terms of their signal-to-noise ratio, they are currently limited to large scale observations with a typical spatial resolution on the order of tens of kilometre. This restricts the applicability of the soil moisture products primarily to hydro-climatological applications (Entekhabi et al., 2008). Active microwave observations acquired via the Synthetic Aperture Radar (SAR) technique are available at a spatial scale (~25 m) suitable also for hydro-meteorological and agricultural applications (Albertson & Parlange, 1999; Entekhabi et al., 2010). Soil moisture retrieval from SAR observations alone is, however, complicated by their sensitivity to surface roughness and vegetation. In order to overcome limitations in deriving accurate soil moisture products at medium to high spatial resolutions, downscaling of accurate passive microwave retrieved soil moisture through high resolution radar observations has been suggested by several authors (i.e. O'Neill et al., 1996, Njoku et al., 2002).

Njoku et al., (2002) demonstrated the retrieval of soil moisture from Passive/Active L-band System (PALS) data collected during the Southern Great Plains Experiment in 1999 (SGP99) using a change detection algorithm. This change detection approach is based on a near linear relationship between radar backscatter/brightness temperature and volumetric soil moisture as discussed by Dobson & Ulaby, (1986) and Njoku & Entekhabi, (1996) and assumes time-invariant surface roughness and vegetation effect on the radar backscatter. Narayan et al., (2006) expanded upon the work of Njoku et al., (2002) by applying the change detection method to Passive/Active L-band System (PALS) and airborne SAR (AIRSAR) from the Soil Moisture Experiment 2002 (SMEX02) campaign conducted in an agricultural setting. Piles et al., (2009) continued the development of the change detection method by applying the algorithm also on the synthetic setting of an Observation System Simulation Experiment (OSSE) for Soil Moisture Active/Passive (SMAP) mission which provided a better quantification of retrieval uncertainties. With the SMAP mission entering its formulation phase, Das et al., (2011) further extended upon previous works as the proposed algorithm for the official SMAP 9-km combined Active/Passive soil moisture product. This algorithm exploits the linear relationship between the time series of radar backscatter and passive microwave soil moisture. The improvement of this approach over the previous methods is that the algorithm provides absolute soil moisture content which is independent of the previous retrievals.

Efforts related to the downscaling of coarse resolution soil moisture retrieved from passive microwave observations is not only limited to the combination with the SAR observations. In fact, the feasibility of utilizing visible and infrared sensors (VIS/IR) observations, as an indirect measure for soil moisture, has been explored in various studies for disaggregating passive microwave soil moisture retrievals. For instance, Chauhan et al., (2003) employed the stochastic relationship between vegetation index, surface temperature and soil moisture for disaggregation to the sub-pixel scale passive microwave observations.

Many studies have utilized this relationship as an approach for downscaling the coarse resolution soil moisture. Recently, this approach has received an increased amount of interest due to launch of the Soil Moisture and Ocean Salinity mission (Merlin et al., (2005-2012) and Piles et al., (2010, 2011)).
The advantage of using active microwave over VIS/IR observations is, however, that the microwave observations of the land surface are available under all weather conditions and are sensitive to soil moisture over the complete dynamic range. Therefore, we adopted for this M.Sc. research the combined active/passive approach of the future Soil Moisture Active and Passive (SMAP) mission. We applied the method described in Das et al. (2011) to the Phased Array type L-band Synthetic Aperture Radar (PALSAR) backscatter data and Advanced Microwave Scanning Radiometer for Earth Observation System (AMSR-E) soil moisture products acquired over the eastern part of the Netherlands.
Similar to the future SMAP mission the PALSAR instrument operated at L-band. As the follow-up of the JERS-1 SAR, PALSAR was launched with Advance Land Observing Satellite (ALOS) in 2006 and ceased operations in May 2011. PALSAR is the only recent L-band SAR system and was capable of providing fully polarized backscatter observations of earth surface at a various spatial and higher temporal resolution (Shimada et al., 2001; Hamazaki, 1999). Jackson et al., 2006 [1] also reported on the potential of PALSAR observations for contributing to the development of future soil moisture missions such as SMAP and ALOS-2.
The AMSR-E is a multi-frequency microwave radiometer with C-band (6.6 GHz) as the lowest frequency. AMSR-E was launched in the 2002 on the Earth Observing System (EOS) Aqua satellite and stopped operating in 2011. From the AMSR-E brightness temperature data sets various operational soil moisture products have been developed (SCI, Jackson, (1993); JAXA, Koike et al., (2004) and Lu et al., (2009); NASA, Njoku et al., (2006); LPRM, Owe et al., (2001, 2008)). For this research, we make use of the data products generated with the Land Parameter Retrieval Model (LPRM, Owe et al., (2001, 2008)) developed jointly by the NASA and Free University of Amsterdam. Rudiger et al., (2009) and Brocca et al., (2011) have compared this soil moisture product to in-situ measurements and found good correlations.
In 2009, the European Space Agency launched the Soil Moisture and Ocean Salinity (SMOS) satellite that measures L-band passive microwave observations, which would have been preferred for this study. However, the presence of Radio Frequency Interference (RFI) in the SMOS soil moisture products acquired over the Twente (Dente et al., 2012) does not allow us to exploit them. It is expected that the difference between the C- and L-band sampling depths will not have a large effect on the results.
The novelty of this research lies in: i) Applying the SMAP algorithm on space borne L-band radar observations and radiometric soil moisture products instead of airborne observations, ii) Utilizing the SMAP algorithm over a heterogeneous landscape.

1.2. Research Objective

The main objective of this study is to retrieve validated soil moisture maps at a medium spatial resolution (1-9 km) in a heterogeneous landscape by combining coarse resolution soil moisture products with high-resolution SAR observations. To fulfil this, AMSR-E soil moisture products from Free University of Amsterdam and NASA (VUA-NASA) and L-band PALSAR are utilized. The soil moisture products are validated against in-situ soil moisture measurements from the network installed in the Twente region.

1.3. Research Questions

- Is it possible to retrieve soil moisture at medium (1-9km) spatial resolution in a heterogeneous landscape by combining coarse passive microwave soil moisture and fine SAR based backscatter observations at the SMAP accuracy requirement (0.04 m^3 m^{-3})?

[1] Source: http://repository.tksc.jaxa.jp/help/pdf/SP-11-007E/pdf/PI028_Thomas_J_Jackson.pdf

- How does the land surface heterogeneity (vegetation, soil type etc.) affect the performance of the retrieval algorithm?
- For which spatial resolution have the soil moisture retrievals the best agreement with the in-situ measurements?

1.4. Anticipated Deliverables

- Validated soil moisture maps at moderate spatial resolution (1-9km) for the Twente region, which can be used for hydro-meteorological and agricultural applications.
- Evaluation of the combined active/passive microwave soil moisture retrieval in anticipated of the launch of NASA's Soil Moisture Active/Passive (SMAP) mission.

1.5. Research Method

We collected the required data set during proposal phase of M.Sc. research as mentioned in follow. First, the availability of ALOS/PALSAR data for the study area was evaluated using the Earth Observation Link (EOLi) Catalogue of the ESA. We selected the Scanning Synthetic Aperture Radar (ScanSAR) mode of PALSAR because of its high temporal resolution in comparison with other modes. To get access to archived PALSAR data set, we submitted a proposal under the Third Party Missions scheme of ESA. The ESA accepted the research plan and granted 50 PALSAR scenes covering the Twente region in the period from May to November 2008 and 2010. As the next step, corresponding descending AMSR-E soil moisture products to PALSAR data set were downloaded from VUA-NASA web page.

Subsequently, correction procedures were applied to PALSAR observations to improve the interpretation of radar backscatters. The Next ESA SAR Toolbox (NEST), which is an open source software, was utilized for performing calibration, antenna pattern removal and co-registration. Speckle noise filtering and incidence angle normalization were approached by writing Interface Description Language (IDL) codes. Then, incidence angle normalization performance on PALSAR backscatters was analysed. Radar backscattering sensitivity to soil moisture variability was also analysed through investigating their response to measured soil moisture and vegetation cover. For this purpose, MODIS Normalized Difference Vegetation Index (NDVI) products were employed as vegetation proxy.

Subsequently, the SMAP algorithm for combined active/passive soil moisture retrieval (Das et al., 2011) was implemented in IDL programming language and applied to the VUA-NASA soil moisture product and the processed PALSAR backscatter data sets. The performance of Active/Passive algorithm was validated via comparison to in-situ measurements[2] at 5 cm depth obtained at the closest time to the PALSAR overpass. A schematization of this research method is presented in Figure 1.1.

[2] Validation was pursued over 2010 since there are no soil moisture measurements during 2008.

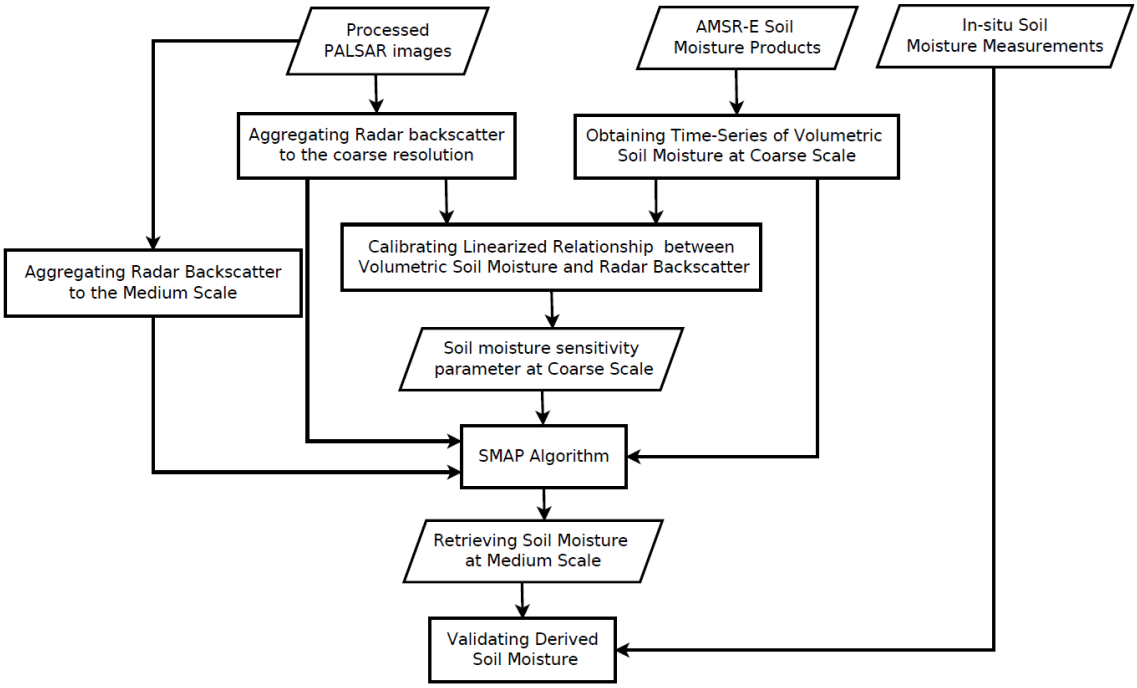

Figure 1.1- The schematic of the procedures taken for combining active/passive microwave observations.

2. STUDY AREA AND IN-SITU MEASUREMENTS

Twente is a region located in the eastern part of the Overijssel Province of the Netherlands (52°05' - 52°27'N latitude and 6°05' - 7°0' E longitude). The topography in Twente is almost flat with elevations varying between -3 m and 50 m above sea level. Land cover is heterogeneous and consists of grassland, agricultural, forested and urban areas. Lying in the temperate zone (according to Köppen Classification System), it experiences mild summers and mild wet winters. December, January and February are the coldest months with average temperatures of 0.5ºC, -0.3ºC and -0.8ºC, respectively. The monthly average air temperature ranges from 3ºC in January to approximately 17ºC in July. Rainfall events are evenly distributed throughout the year resulting in an annual sum of about 765 mm on average.
Twente region has four main soil types, including sandy soils, loamy soils, manmade sandy thick earth soils and peat soils covered by a layer of peat or sand. At the near surface soil layer, however, the soil is sand and loamy sand.

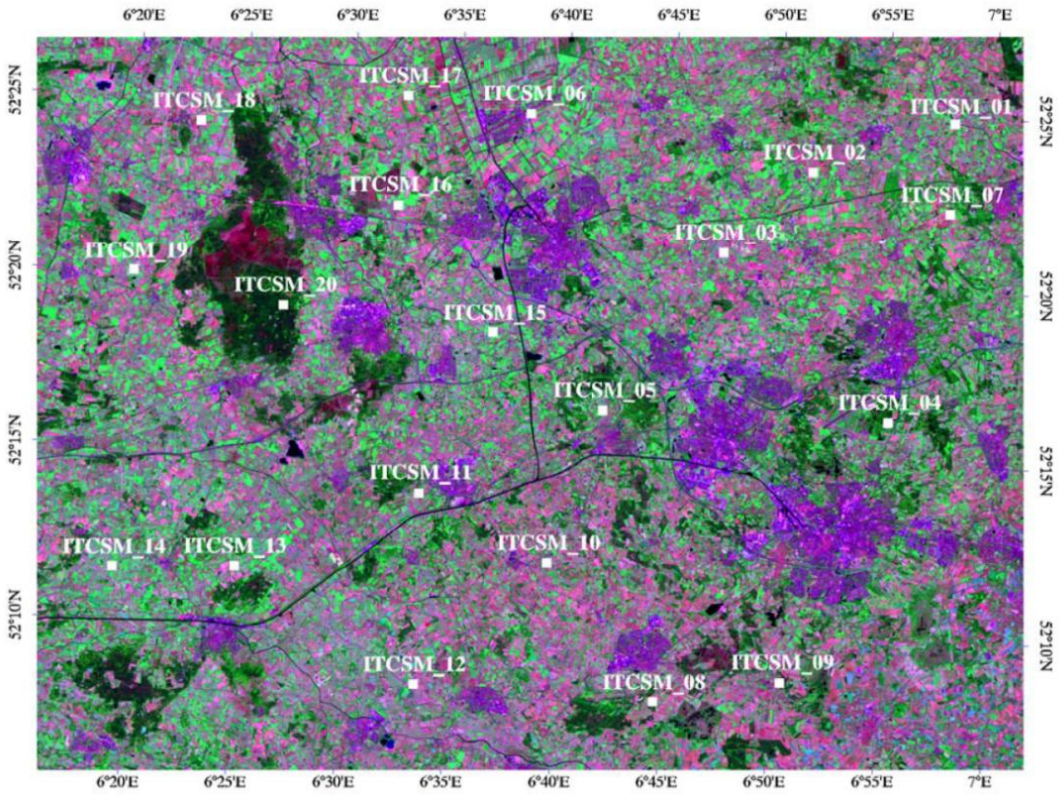

Figure 2.1- Location Map of the Twente region and soil moisture stations shown with white squares[3].(Landsat 5 TM image (RGB: band7, band 4, band 2) acquired at 27th of June 2010; Forested area in dark green, Urban area in purple, Grassland in light green and Corn fields in pink)

Since September 2009, Twente area is equipped with EC-TM ECH2O probe[4] network that records soil moisture and temperature observations every 15 minutes. the installed network has 20 stations covering an

[3] Source : http://www.itc.nl/library/papers_2011/scie/dente_twe.pdf

[4] The EC-TM ECH_2O probe is a capacitance sensor measuring the dielectric permittivity of the soil that should be converted to volumetric soil moisture by standard calibration equation.

area of approximately 50 km × 40 km. one station is installed in forested area, sixteen stations are located in a grassland environment and three in corn fields. The faculty of geo-information science and earth observation of the University of Twente, Netherlands provided this data set. Dente et al. (2012) also used this data set for evaluating the accuracy of SMOS soil moisture estimates over the Twente.

Rainfall data is provided by the water board of Regge and Dinkel, the authority of managing the Twente region's water quality and quantity. The water board determines the amount of occurring rain events through a network with 18 stations covering the area. These stations are equipped with automatic rain gauges recording the rainfall at a time interval of 20 minutes.

3. REMOTE SENSING DATA SETS

3.1. AMSR-E VUA-NASA Soil Moisture Product

AMSR-E daily level-3 volumetric soil moisture products were used for this study. This data set is available in a global cylindrical EASE-Grid at 25 km resolution. AMSR-E soil moisture products are produced by applying the Land Parameter Retrieval Model (LPRM) developed by Owe et al., (2001 & 2008) to the passive microwave measurements from the AMSR-E instrument on board of the NASA EOS Aqua satellite (Figure 3.1). This algorithm employs radiative transfer model describing soil and vegetation microwaves emissions. The advantage of the LPRM algorithm is that no in-situ measurements are required for the calibration of parameters.

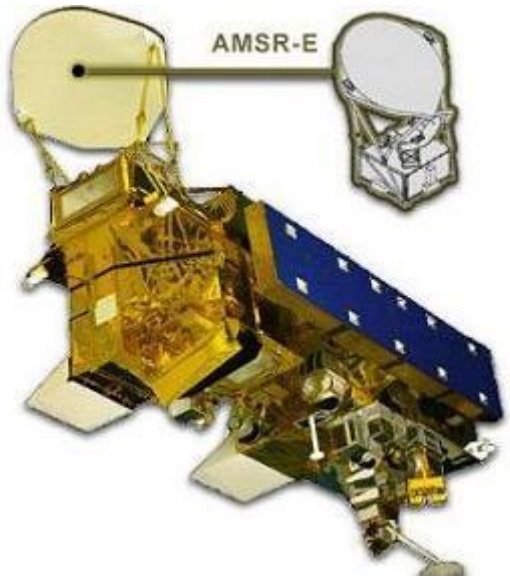

Figure 3.1- AMSR-E instrument on board of the Aqua satellite[5]

Descending AMSR-E soil moisture data set (obtained at 01:30 A.M. local time) was chosen because of their more accurate observation of soil moisture (e.g. Draper et al., 2009; Jackson et al., 2010; Su et al., 2011). This data set is available free of charge at (http://www.falw.vu/~jeur/lprm). Several studies, such as Schumann et al., (2009) and Miralles et al., (2011) have also used this soil moisture product for deriving root-zone soil moisture and estimating daily evaporation, respectively.

3.2. Phased Array type L-band Synthetic Aperture Radar (PALSAR) data

PALSAR instrument carried on ALOS satellite is an L-band SAR system operating at multiple polarization and imaging modes (single, dual, polarimetric and scanning synthetic aperture radar). These different modes can provide SAR backscatter (σ°) observations in multiple image swaths (30-350 km) at various spatial resolutions (10-100 m) at revisit times varying from 2 days up to 46 days. In the ScanSAR mode single polarized σ° data is collected over a 350 km swath width with a spatial resolution of 100 m every 2-5 days. Radiometric accuracy of ScanSAR mode is reported to be better than 1 dB in Shimada et al., (2009) and Ito et al., (2001). A total of 40 PALSAR ScanSAR scenes are available for the study area, which were acquired in 2008 and 2010 from May to November. The PALSAR data sets were delivered by the ESA as

[5] Source : http://wetlands.jpl.nasa.gov/instruments/index.html

level 1.5 products. Appendix 1 gives basic information (date, track, pass) on the available scenes. More detailed information related to characteristics of PALSAR ScanSAR mode is shown in Table 3.1.

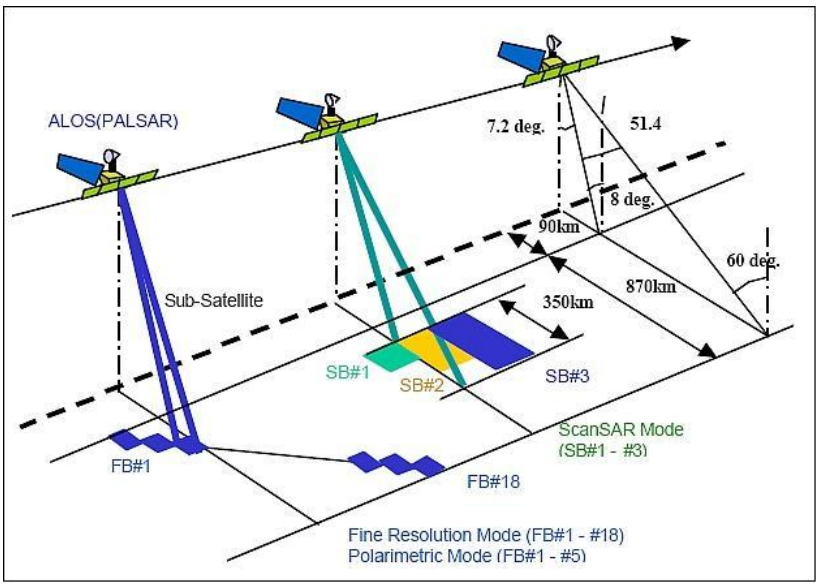

Figure 3.2- Illustration of PALSAR observation modes[6]

Table 3.1- The PALSAR ScanSAR mode Characteristics

Mode	ScanSAR (WB1)
Central Frequency	1.27 GHz
Polarization	HH
Spatial Resolution	100 m (Multi Look)
Off-nadir Angle	20.1 ° – 36.5 °
Incidence Angle	18 ° - 43.3 °
Orbit Acquisition	Ascending/Descending
Overpass Time	Ascending: around 10:30 p.m. Descending: around 10:30 a.m.
S/N	< -23 dB

3.3. MODIS Normalized Difference Vegetation Index (NDVI) Product

MODerate-resolution Imaging Spectroradiometer (MODIS) on board of NASA's Terra satellite measures radiation emitted or reflected by surface in the optical and thermal part of the electromagnetic spectrum. From the MODIS data sets various land surface products are derived. An example is the Normalized Difference Vegetation Index (NDVI) product named MOD13A2, which is a 16-day composite and available at a 1 km resolution. The 16-day composite are derived from daily surface reflectance product (MOD9) (Huete et al., 2002). Free access to MODIS VI products in the Hierarchical Data Format-Earth Observing System (HDF-EOS) format is possible from the following webpage http://glovis.usgs.gov.

[6] Source : https://directory.eoportal.org/web/eoportal/satellite-missions/a/alos

4. METHODOLOGY

4.1. PALSAR Image Processing

The following pre-processing steps were applied to PALSAR data sets:

- Antenna pattern removal and calibration
- Co-registration
- Speckle noise filtering

Each of the processing steps is briefly described in the text below.

Antenna Pattern Removal and Calibration

Received power and σ° are sensitive to range and incidence angle variation, respectively. This sensitivity leads to weak grey repercussion of the targets across the image (Ulaby et al., 1982) and wide fluctuation of received signals. To moderate the range and angular impact on PALSAR signals, receiver gain was adjusted by utilizing Remove Antenna Pattern tool of the NEST software. This technique considers receiver gain even as a function of incidence angle variation and/or time delay.
To pursue quantitative analysis on SAR observations, calibration was applied to PALSAR images. Calibration converts intensity to σ° in dB which directly represents the scene backscattering. This process also makes obtained SAR signals ready for utilization in the soil moisture retrieval algorithm.

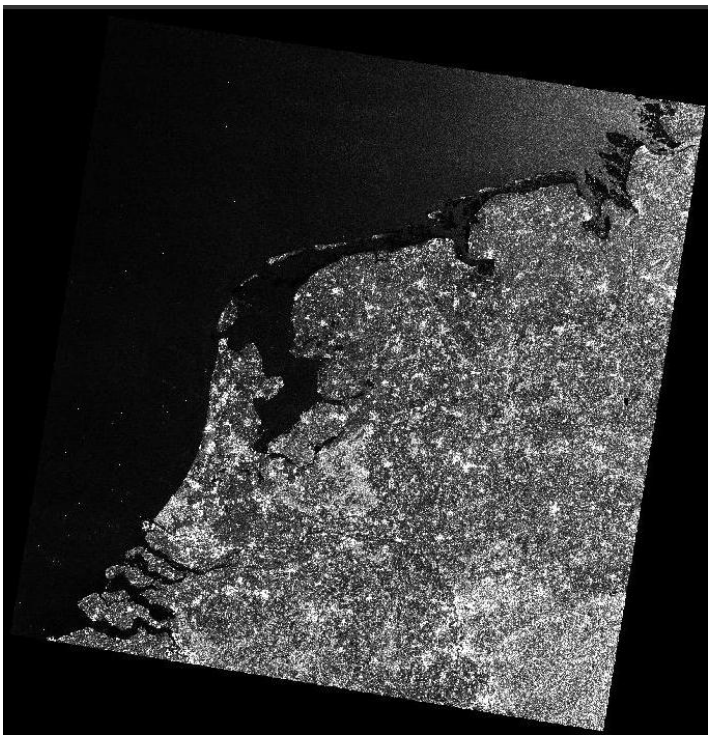

Figure 4.1- PALSAR ScanSAR mode image acquired at 8/6/2008, after Antenna pattern removal.

Co-registration

Multi-temporal images produced by PALSAR ScanSAR mode suffer from geometric differences. This discrepancy can be the result of different orbits (Appendix 1) of PALSAR sensor over the same region. Accordingly, we registered PALSAR images which were taken at different dates by utilizing NEST's co-

registration tool. This process in NEST is based on the correlation method choosing Ground Control Points (GCPs) automatically from the master and slave images.

Speckle Noise Filtering

Speckle noise exists in Synthetic Aperture Radar (SAR) images that causes higher or lower brightness value of the pixel in contrast to neighboring pixels (Xia & Sheng, 1996). This granular noise is the result of intrferrence between returned microwaves radiation scattered from the individual scatterers. The available filtering techniques can be classified in three main groups, namely, multiple look processing, adaptive filters and non-adaptive filters. Non-adaptive median filter by kernel window size of 5x5 applied in Thoma et al., (2008) and Van der Velde et al., (2012a) was approached on PALSAR σ°. The advantage of median filter lies in preserving the edges between features while it supresses the speckle noise (Qui et al., 2004).

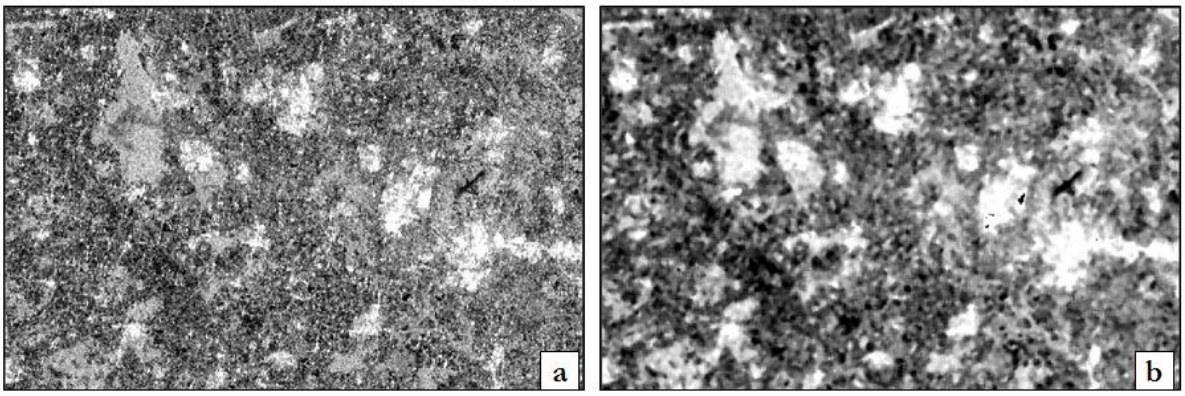

Figure 4.2- Filtering process impact on the image acquired at 8/6/2008, a) raw backscatter, b) Median filter with kernel window size of 5x5.

Incidence Angle Normalization

Wave properties such as the incidence angle resulted from the side-looking configuration of the SAR sensor disturbs in interpretation of the backscattering values. Obtaining radar backscatters depending only on the surface properties requires the minimization of observation geometry effect. Consequently, incidence angle normalization toward a single reference angle should be done. This leads to more accurate quantitative analysis of retrieved radar backscattering coefficients (Löw et al., 2005).

We normalized the σ° based on the physical model of Lambert's law for optics assuming the cosine relationship between the incidence angle and amount of scattering per unit of surface area. Van der Velde et al., (2008), Van der Velde & Su, (2009) and Lievens et al., (2011) also utilized this method for incidence angle correction. The backscatter observations were normalized to a reference angle of 30 degrees being averaged incidence angle (Ulaby et al., 1982; Wagner et al., 1999) in the PALSAR data set,

$$\sigma^{\circ}\left(30^{\circ}\right) = \frac{Cos^2\left(30^{\circ}\right)}{Cos^2\left(\theta_i\right)}\,\sigma^{\circ}\left(\theta_i\right) \tag{4.1}$$

Where, $\sigma^{\circ}(\theta_i)$ is the incidence angular dependent radar backscatter, θ_i represents the local incidence angle and $\sigma^{\circ}(30^{\circ})$ is the normalized backscatter to a single incidence angle of 30 in degree.

4.2. Soil Moisture Retrieval Algorithm

Absolute values of soil moisture contents at medium scale were estimated through application of the change detection algorithm by Das et al., (2011). The combined active/passive soil moisture retrieval with this algorithm is based on the linearized relationship between volumetric soil moisture and L-band radar backscatter observations (e.g. Kim & van Zyl, 2009). Using this approach, time series of accurate

volumetric soil moisture retrieved from passive microwave observations was combined with observed co-polarized radar backscatter aggregated to an intermediate spatial scale. Aggregation of the fine spatial resolution backscatter to the medium scale is needed to suppress the speckle noise. Before aggregation, Obtained backscatter signals over the residential region were excluded by masking out the urban area (wood et al., 1993) due to their interference in soil moisture estimation.

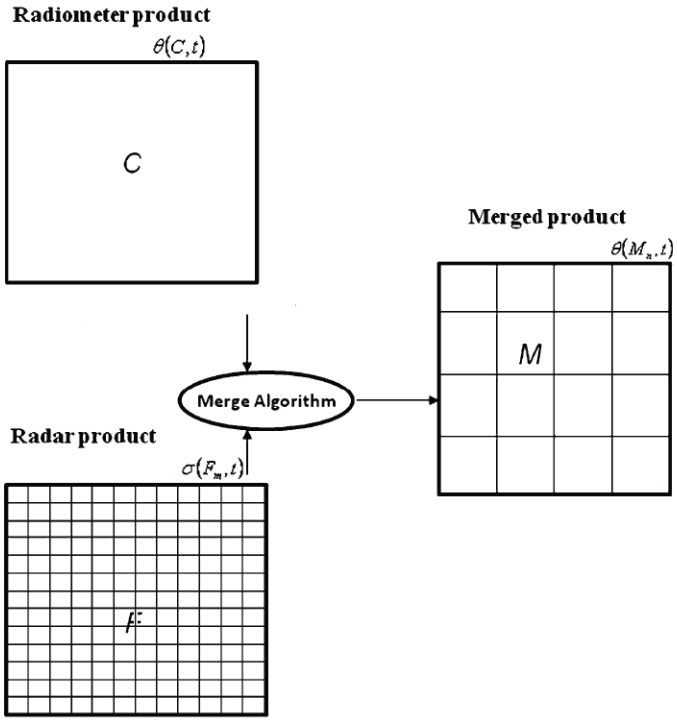

Figure 4.3- Grid topology of radiometric product at coarse resolution (C), radar product at fine resolution (F) and merged product at medium resolution (M). [7]

Soil moisture retrieval approach utilized in our study is visualized in Figure 4.3 and can mathematically be formulated as follows,

$$\theta_m = \theta_c + \beta_c \left(10 * log\left(\overset{\circ}{\sigma_m}\right) - 10 * log\left(\overset{\circ}{\sigma_c}\right)\right) \quad (4.2)$$

Where θ is volumetric soil moisture ($m^3.m^{-3}$), β is an empirical parameter describing soil moisture sensitivity of σ°, σ° is co-polarized radar backscatter and subscripts m and c indicate the variable is representative for either the medium or coarse spatial scale, respectively.
The soil moisture at the coarse spatial scale is obtained from the passive microwave soil moisture product. The parameter β follows from the linear relationship between the θ_c and backscatter aggregated to the coarse spatial scale (σ°_c) that should be established with a θ_c and σ°_c time series and can be expressed as,

$$\theta_c = \alpha_c + \beta_c * \left(10 * log\left(\overset{\circ}{\sigma_c}\right)\right) \quad (4.3)$$

Here, a_c is a calibrated parameter depending on vegetation cover, vegetation type and surface roughness. a_c has been assumed to be homogenous at coarse scale.

[7] Adapted from Das et al. 2011

5. ANALYSIS OF PALSAR OBSERVATIONS AND AMSR-E DATA

5.1. Backscatter Analysis

5.1.1. Incidence Angle Normalization

For compensating the impact of incidence angle as wave property on SAR data, incidence angle normalization based on Lambert's law was applied. Through this processing step, backscatter values over the image swath were normalized towards a reference angle of 30 degrees.

Figure 5.1 presents the speckle-filtered and angle-normalized σ° against local incidence angle for different land covers (grassland, corn field and forested area). The figure illustrates that the response of the L-band σ° to incidence angle is small for each of the three selected land-covers. Furthermore, it shows the low impact of angular correction on the σ°. This is consistent with the work from Menges et al., (2001) which demonstrated that there is a slight change in angular responses of L-band σ° after incidence angle correction. Even though the angular response of the σ° is not significant, the normalization further suppresses the σ° change as a function of incidence angle.

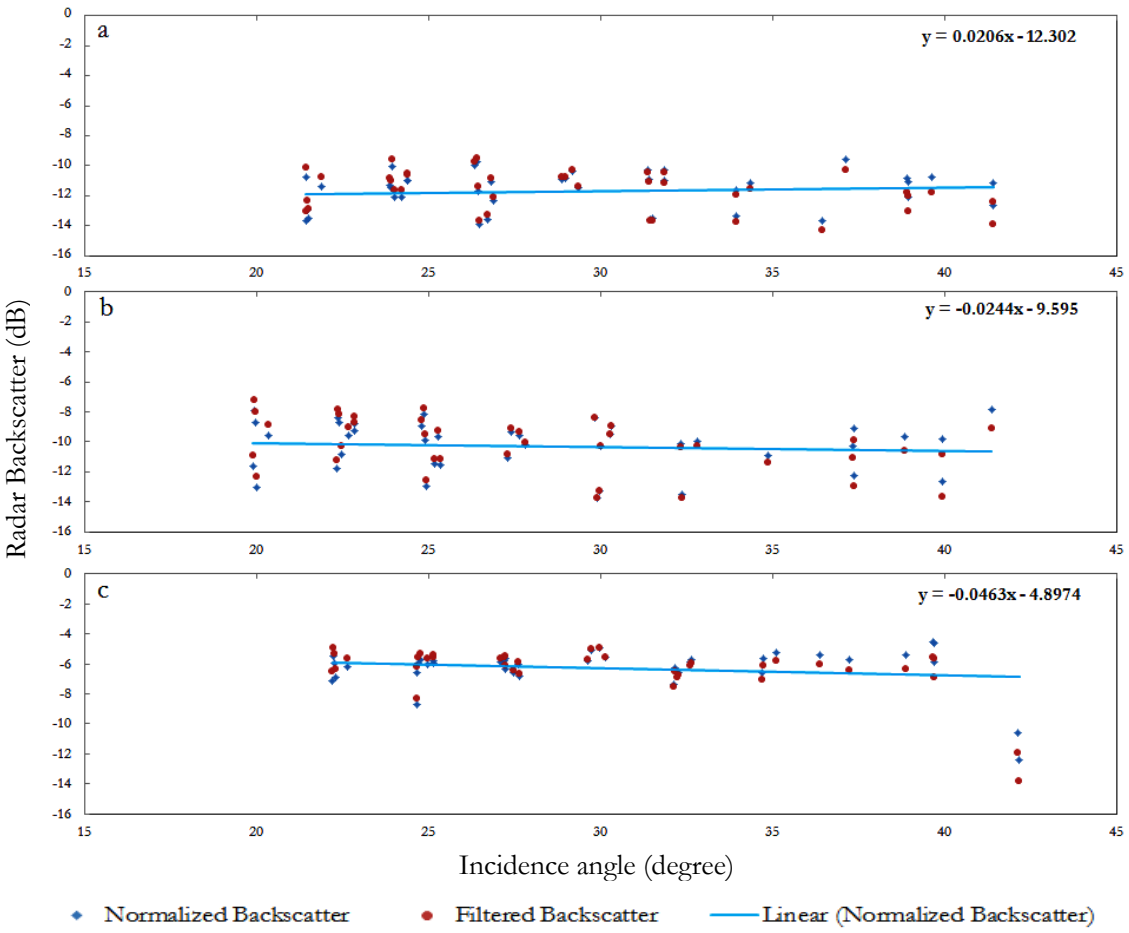

Figure 5.1- Illustrating the speckle-filtered and angle-normalized σ° against the local incidence angle variation over 500 ×500 m2 area of a) grassland (ITCSM15), b) corn field (ITCSM08) and c) forested area (ITCSM20).

5.1.2. Response to Soil Moisture and NDVI

Many studies (i.e. Dobson & Ulaby, 1986; Njoku et al., 1996; Kim & Van Zyl, 2009; Das et al., 2011) have previously reported on a near linear relationship existence between σ° and soil moisture. Figure 5.2 shows the linear relationship between the PALSAR σ° and measured volumetric soil moisture for a typical grassland, corn field and forested area in the study area. Indeed, well defined linear relationships are observed for the grassland and corn field resulting in coefficient of determination (R^2) of 0.69 and 0.66, respectively. Based upon previous investigation these results are expected (Joseph et al., 2010). Over the forested area the relationship between σ° and soil moisture is much weaker. This can be explained by the fact that the forest biomass attenuates most of the signals coming from the soil (Ferrazzoli & Guerriero, 1995; Saatchi et al., 2007). In addition, high values of PALSAR σ° are captured over forest. Moderate and low σ° are collected over grassland and cornfield, respectively which is not surprising as corn field is much more vegetated than grassland. These results are consistent with the found strong correlation between biomass and radar backscatters at lower frequencies in Dobson et al., (1992).

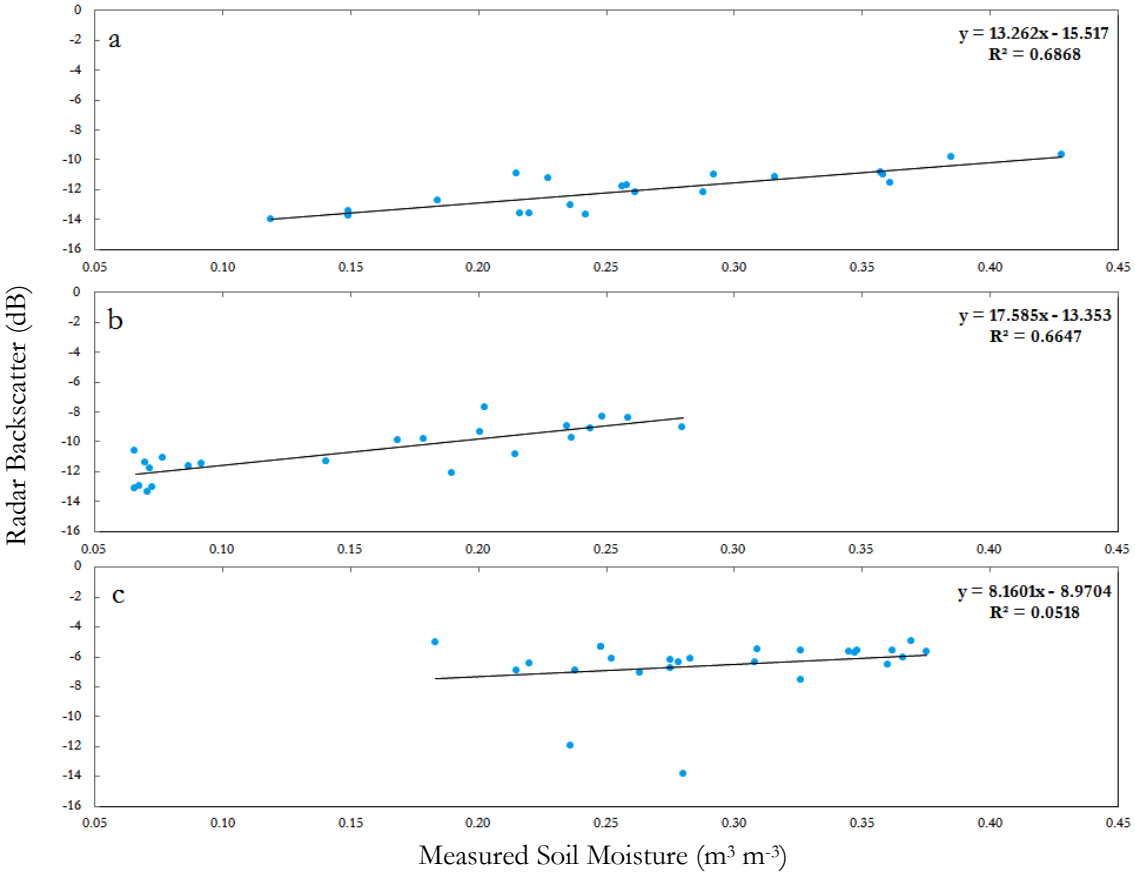

Figure 5.2- Plotted normalized σ° against measured soil moisture contents over different land covers including a) grassland (ITCSM15), b) corn field (ITCSM08) and c) forested area (ITCSM20).

Time series of rainfall and NDVI is plotted on top of the soil moisture and backscatter cross section in Figure 5.3. This plot highlights the σ° variations in response to land surface conditions. The figure illustrates the expected hydrological behaviour; whenever rain is absent also the soil moisture content decreases. The σ° signals from the grassland and corn field which are in good agreement with measured soil moisture (Figure 5.2) also show the same response to the seasonal variability of rainfall. This relationship is specially visualized over grassland during June and July which experience longer period without any rain.

For further analysis on PALSAR σ°, NDVI as an indicator for biomass variations was employed. Figure 5.3 displays approximately steady behaviour of NDVI during spring and summer. This constant behaviour is in agreement with findings by Nicholson et al., (1990). He mentioned that NDVI will remain stable when the plant reaches to its maximum level of photosynthetic capacity. This observation, therefore, shows that NDVI cannot be useful for identifying vegetation effect on the σ° responses.
Based on the mentioned observations, rainfall and subsequently soil moisture are the main land surface conditions affecting the PALSAR σ° variability (e.g. Van der Velde, 2010). This explains the sensitivity of PALSAR ScanSAR mode to the soil moisture content and confirms the potential of PALSAR data sets for soil moisture mapping.

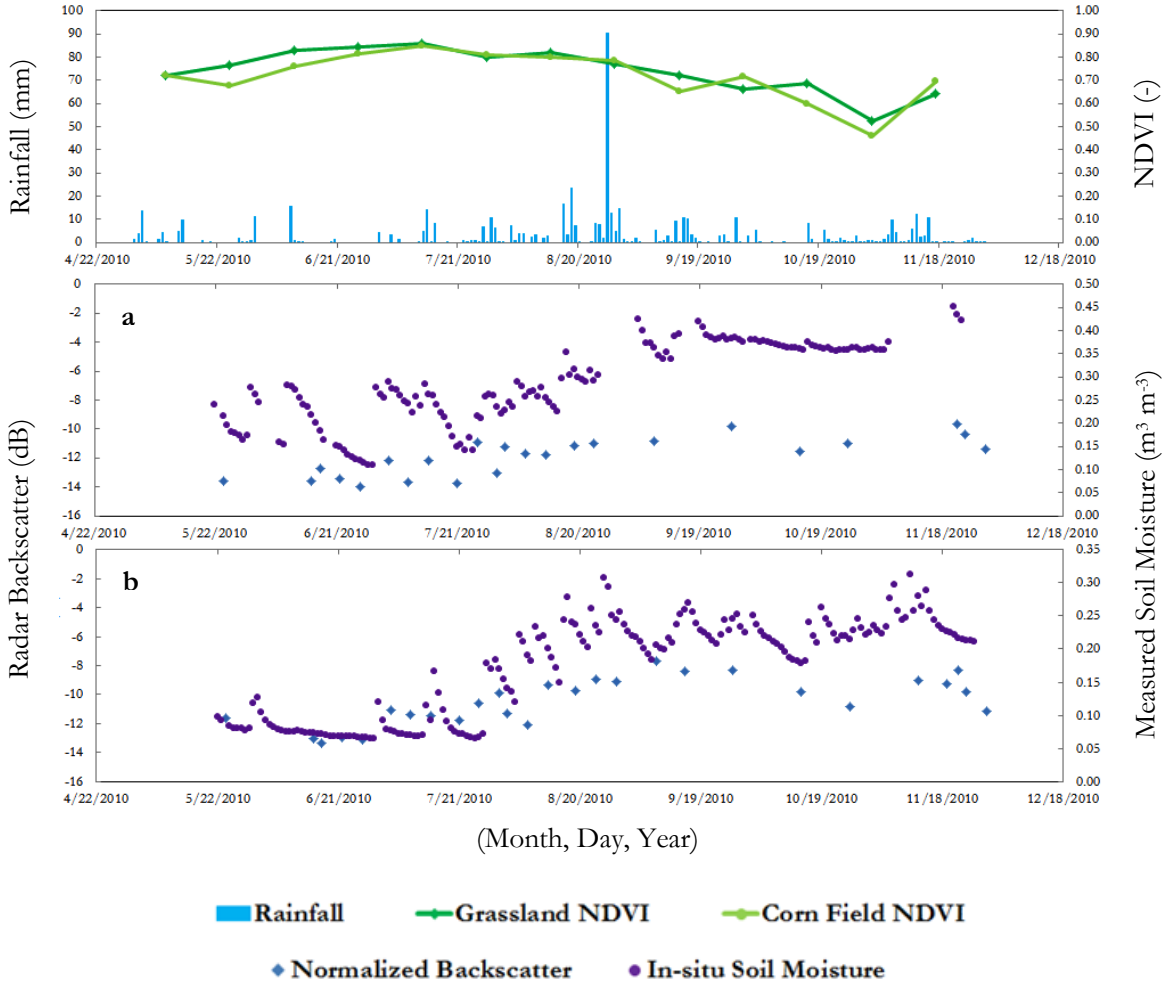

Figure 5.3- Temporal variability of rainfall, NDVI, soil moisture and incidence angle normalized σ° over 500 × 500 m² areas of a) grassland (ITCSM15), b) corn field (ITCSM08).

5.2. VUA-NASA AMSR-E Product Validation

In this section, descending LPRM soil moisture products are validated against in-situ measurements at two scales. First, satellite observations are compared against the individual stations. Then, AMSR-E retrievals are compared to the mean soil moisture averaged over all stations within a grid cell. From the matchups the bias, coefficient of determination (R^2), Root Mean Square Error (RMSE) and Mean Absolute Error (MAE) are calculated. Table 5.1 lists the statistics from the comparisons. It should be noted that stations ITCSM14 and ITCSM16 were not included in validation as they did not provide consistent measurements.

Table 5.1- Statistical analysis of LPRM soil moisture validated against,

a)Individual stations within the AMSR-E grid,

Stations	Land Cover	R^2	Bias	RMSE	MAE
ITCSM01	Grass bush	0.59	0.04	0.084	0.071
ITCSM02	Grassland	0.53	0.207	0.214	0.207
ITCSM03	Grassland	0.48	-0.01	0.052	0.041
ITCSM04	Grassland	0.64	0.1	0.115	0.1
ITCSM05	Grassland	0.36	0.171	0.182	0.171
ITCSM06	Grassland	0.52	0.136	0.149	0.136
ITCSM07	Corn Field	0.54	0.119	0.127	0.119
ITCSM08	Corn Field	0.41	0.179	0.189	0.18
ITCSM09	Corn Field	0.35	0.147	0.162	0.147
ITCSM10	Grassland	0.56	0.034	0.071	0.057
ITCSM11	Grassland	0.39	0.069	0.093	0.071
ITCSM12	Grassland	0.53	0.195	0.202	0.195
ITCSM13	Grassland	0.24	0.173	0.183	0.172
ITCSM15	Grassland	0.37	0.074	0.098	0.076
ITCSM17	Grassland	0.41	0.245	0.25	0.245
ITCSM18	Grassland	0.24	0.18	0.196	0.18
ITCSM19	Grassland	0.54	0.11	0.131	0.115
ITCSM20	Forest	0.59	0.07	0.079	0.07

b) mean soil moisture averaged over all stations within a grid cell of AMSR-E; n is the number of stations within each AMSR-E grid scales

Pixels	R^2	Bias	RMSE	MAE	n
0,0	0.59	0.11	0.123	0.11	3
1,0	0.52	0.157	0.164	0.157	4
2,0	0.64	0.124	0.131	0.124	5
0,1	0.24	0.173	0.184	0.173	1
1,1	0.63	0.118	0.126	0.118	4
2,1	0.35	0.147	0.162	0.147	1

The assessment of the LPRM soil moisture products results in R^2 varying from 0.24 to 0.64 for both comparisons with individual measurements as well as grid-cell averaged soil moisture values. This is comparable to the results found by Draper et al., (2009), Gruhier et al., (2010) and Jackson et al., (2010) who compared LPRM product to in-situ measurements over various climatological conditions. For instance, Draper et al. validated LPRM products over Australia and reported on correlations (R) ranging from 0.67 to 0.92; equivalent to R^2 values of 0.45 and 0.85, respectively. The LPRM validation in Gruhier et al. was pursued over low vegetated and homogenous area in Mali. They compared LPRM products to up-scaled in-situ measurements and found R (R^2) equal to 0.89 (0.79), 0.58 (0.34) and 0.60 (0.36) for two years period, monsoon season and dry season, respectively.

We obtained lower R^2 in contrast to previous studies, which can be argued that study area includes significant portion of forested and urban areas. The effect of urban structure is visible in the found relationships. For instance, for pixel (2,1) low R^2 is obtained whereas this pixel is covered by the largest urban faction (~ 40%). Results from the LPRM validation against individual stations, somewhat surprising

show that one of the best agreements is found for the forested site. The soil moisture dynamics in the sampled forest represents apparently the AMSR-E footprint quite well.
Based on the results presented in Table 5.1, in general, high values of positive biases are obtained between the LPRM products and in-situ measurements. The large bias is a well-known problem for LPRM products and has previously been identified in Jackson et al., (2010) and Wagner et al., (2007). The presence of bias explains also the large RMSE values.

6. RESULTS

6.1. PALSAR σ° versus AMSR-E Soil Moisture

In essence, soil moisture sensitivity parameter (βc) in the SMAP Active/Passive algorithm is calculated via calibration between, in this case, the LPRM volumetric soil moisture and PALSAR σ° aggregated onto AMSR-E grid. Figure 6.1 presents the relationship between LPRM soil moisture and PALSAR σ° determined at 5% level of uncertainty. According to this figure, slope varies from 0.0291 to 0.041 ($m^3\ m^{-3}$ /dB). Obtained slopes show the appropriate sensitivity of σ° to the temporal variability of LPRM because changes in the soil moisture of about 0.1 $m^3\ m^{-3}$ coincides with an average change of 3 dB in σ°.

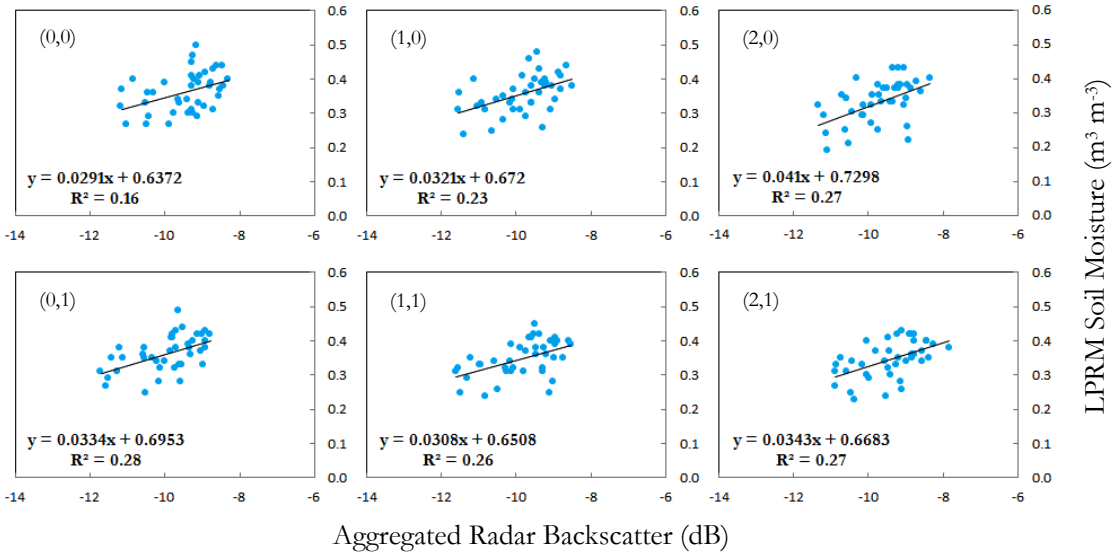

Figure 6.1- Scatter plot of LPRM soil moisture versus PALSAR σ° aggregated onto AMSR-E grid for each pixel.

6.2. Validation

The SMAP algorithm described in chapter 4 was applied to LPRM soil moisture-PALSAR σ° pairs to estimate soil moisture at medium resolution. Soil moisture contents were produced at two resolutions equal to 1 and 5 km in order to figure out the algorithm performance when different level of speckle noise exists in PALSAR σ°. The quality of these products is assessed by comparing both retrievals with in-situ measurements from individual stations. From the matchups the bias, coefficient of determination (R^2), Root Mean Square Error (RMSE) and Mean Absolute Error (MAE) are calculated. These results are presented in Appendix 2 and Table 6.1 includes calculated mean and standard deviation (Std. Dev.) for the statistical parameters. It should be noted that this comparison is limited to 2010 because the Twente network started to record soil moisture since 2009.

Table 6.1- Statistical analysis of soil moisture retrievals from combination of LPRM products and PALSAR σ°

Soil Moisture Retrievals scale	R^2		Bias		RMSE		MAE	
	Mean	Std. Dev.	Mean	Std. Dev.	Mean	Std. Dev.	Mean	Std. Dev.
1 km	0.42	0.124	0.076	0.094	0.125	0.044	0.109	0.046
5 km	0.46	0.14	0.161	0.204	0.138	0.05	0.126	0.052

R^2 varies generally from 0.11 to 0.69 (see Appendix 2) for soil moisture retrievals at the resolutions of both 1 and 5 km. This broad variation explains the large standard deviation of R^2 presented in Table 6.1. Obtained range of R^2 is in some extent similar to the LPRM, however, for some stations applied algorithm has reduced R^2. This reduction is more pronounced in 1 km retrievals. For instance, at station ITCSM11 the R^2 reduces by more than 70%. Reduction in R^2 may be attributed to the spatial miss-match between the retrievals and in-situ measurements. In general, spatial miss-match is expected to be more for the both retrievals as compared with LPRM products at coarse resolution. Patchiness in surface roughness is also more evident in finer resolutions which may result in reduction of R^2. Figure 6.2 presents scatter plots of retrieved θ against measured θ, as an example, for six stations. These stations are selected in such way that the lowest, moderate and best agreement between estimated and measured θ is demonstrated for both resolutions.

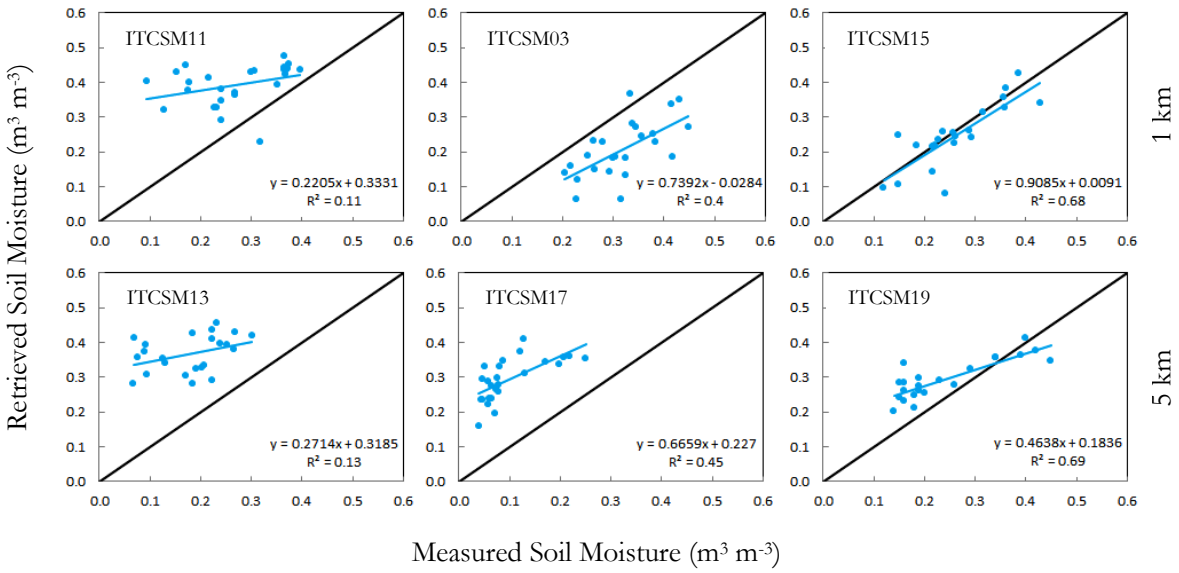

Figure 6.2- Retrieved soil moisture versus measured soil moisture from typical sites over grassland

Table 6.1 lists calculated biases of on average 0.076 and 0.161 for retrievals at 1 and 5-km, respectively. Based on the fact that accuracy of radiometer-only products influences the accuracy of outputs from the SMAP algorithm (Das et al. 2011), these positive biases are expected because LPRM products systematically overestimate the measured θ as is also shown in section 5.2. The presence of this bias also increases the other error statistics (MAE and RMSE). In essence, the existence of the bias does not restrict the applicability of the resulting soil moisture products because different hydro-meteorological models inevitably produce different climatologies (Koster et al., 2009; Van der Velde et al., 2012b). In many data assimilation applications prior bias corrections are common practice (Reichle, 2008).

Here, the bias is removed by using simple difference-based method (Berg et al., 2003) in which the calculated bias is subtracted from retrieved θ. Table 6.2 presents the error statistics (R^2, RMSE, MAE). This procedure reduced both RMSE and MAE by approximately 50%. In addition, bias removal has declined the RMSE fluctuation. For instance, wide range of RMSE (5.3%-22.8% volumetric soil moisture) for products at 1-km has lowered to 4.2% - 8.6% after bias correction. Obtained RMSE range after removing the bias is similar to the possible accuracy for the 1-km Sentinel-1 soil moisture products reported by Wagner et al., (2009).

Averaged RMSE's of 0.068 and 0.058 $m^3 m^{-3}$ are obtained at 1-km for the former and 5-km for the later, after bias correction. Calculated accuracy indicates that SMAP soil moisture retrievals do not meet the SMAP accuracy requirement of 0.04 $m^3 m^{-3}$. However, applied algorithm could derive reasonably accurate

soil moisture with respect to the accuracy of SAR-based soil moisture products (~0.06 m^3 m^{-3}) (e.g. Satalino et al., 2002; Mattia et al., 2010; Van der Velde et al., 2012a).

Table 6.2- Statistical analysis of soil moisture retrievals from combination of LPRM products and PALSAR σ° after bias correction

Soil Moisture Retrieval scale	R^2		RMSE		MAE	
	Mean	Std. Dev.	Mean	Std. Dev.	Mean	Std. Dev.
1 km	0.42	0.124	0.068	0.011	0.054	0.01
5 km	0.46	0.14	0.058	0.01	0.047	0.01

The performance of the SMAP is compared to the LPRM product by taking the ratio of their respective error statistics (R^2, RMSE, MAE). This comparison was carried out only for pixel (2,0) of AMSR-E and the stations falling in it because it has the most stations. It should be noted that the utilized LPRM error statistics are recomputed after bias correction (see Appendix 4). Table 6.3 presents these ratios for both SMAP retrievals at 1-km and 5-km resolution. Obtained ratios demonstrate that applied algorithm has led to reduction of R^2 and increase in the RMSE for both products. Consequently, it is concluded that SMAP products have no improvement over the LPRM in terms of their accuracy.

Increased RMSE for SMAP products in contrast to LPRM products is comparable to earlier studies by Das et al., (2011) and Piles et al., (2009). They both confirmed that applied SMAP algorithm on the airborne and synthetic data sets successfully increases the accuracy of products. Das et al. reported on RMSE improvements of 0.015-0.02 cm^3cm^{-3} for the retrievals at 9-km resolution, while without aggregating σ° to the 9-km resolution the accuracy did not improve as compared to the radiometer-only performance. For practical reasons the medium resolutions defined for this research are chosen to be 1-km and 5-km, which may partly explain the increase in error statistics as compared to the coarse resolution products. It should, however, be also noted that both Das et al. and Piles et al. made use of airborne and synthetic datasets, which constructed for idealized conditions (i.e. radiometric accuracy and prescribed roughness, vegetation). Hence, the somewhat larger error statistics found in this study can be argued for given the fact that only satellite data is used and the patchiness of the study area. Due to dependency of soil moisture sensitivity parameter (β) to the vegetation and surface roughness, β varies widely over a heterogeneous landscape. However, the SMAP algorithm is developed upon assuming β as a homogeneous parameter within radiometer footprint. This assumption is the main source of error in the algorithm performance (Das et al., 2011 and Piles et al., 2009) especially over the heterogeneous landscape as the Twente region.

Closer look at the obtained ratios shows better performance of the SMAP algorithm at 5-km. Obtained discrepancy in the retrievals accuracy can be explained by radar speckle noise. The speckle noise, in general, is suppressed by averaging over more independent samples and, thus, producing a coarse resolution. Consequently, lower noise level exists in 5-km resolution than 1-km resolution which results in lower errors of estimation and this finding is in agreement with Das et al., (2011).

Table 6.3- Calculated ratios between error statistics of bias corrected retrievals and LPRM products

	Soil moisture at 1 km			Soil moisture at 5 km		
Station	R^2	RMSE	MAE	R^2	RMSE	MAE
ITCSM01	0.83	1.81	1.94	0.97	1.64	1.88
ITCSM02	0.44	1.81	2.00	0.88	1.24	1.34
ITCSM03	0.63	1.52	1.56	0.83	1.19	1.19
ITCSM04	0.58	1.76	1.91	0.81	1.55	1.59
ITCSM07	0.83	1.57	1.66	0.70	1.17	1.19

6.3. Soil Moisture Maps

The reliability of the produced soil moisture contents is described above. For studying the temporal and spatial performance of the applied algorithm, series of soil moisture maps are presented in Figure 6.3 and 6.4 for retrievals at 1-km and 5-km resolution, respectively.

Based upon both series of soil moisture maps, applied algorithm significantly has improved the spatial distribution of the soil moisture within the AMSR-E footprint. Captured variation of soil moisture is also consistent with landscape heterogeneity of the study area, especially at 1-km resolution. Lower amount of soil moisture, for instance, is expected in agricultural regions due to occurrence of higher evaporation from top of the soil surface, which is shown in the produced maps at 1-km. These results, in general, confirm the success of algorithm in retrieving spatial variability of soil moisture at finer resolution.

Temporal dynamics of regional soil moisture is well reflected by both products in such way that lower and higher soil moisture contents are captured during first and second half of the year, respectively. Even occurrence of drought across the study domain is presented in both products. However, each product detects a different duration and intensity of drought. Soil moisture retrievals at 1 km demonstrate severe drought condition with soil moisture levels up to 0.03 m^3 m^{-3} over a long period in May-July 2010, whereas only slightly lower soil moisture levels (0.14 m^3 m^{-3}) are observed in the 5-km products. The general soil moisture patterns coincide with a reduction of rainfall during the same period (Figure 5.3).

Closer look at the Figures 6.3, 6.4 and 5.3 shows also that the temporal soil moisture evolution retrieved at a 1- km resolution has a much better agreement with rainfall pattern. From the difference between soil moisture snapshots acquired at 06/17/2010 and 06/27/2010, for instance, absence of rainfall has resulted in more temporal variability of regional soil moisture at 1-km. These observations are in line with our understanding of the correlation between the spatial and temporal scale of soil moisture as Vinnikov et al., (1996) has previously described.

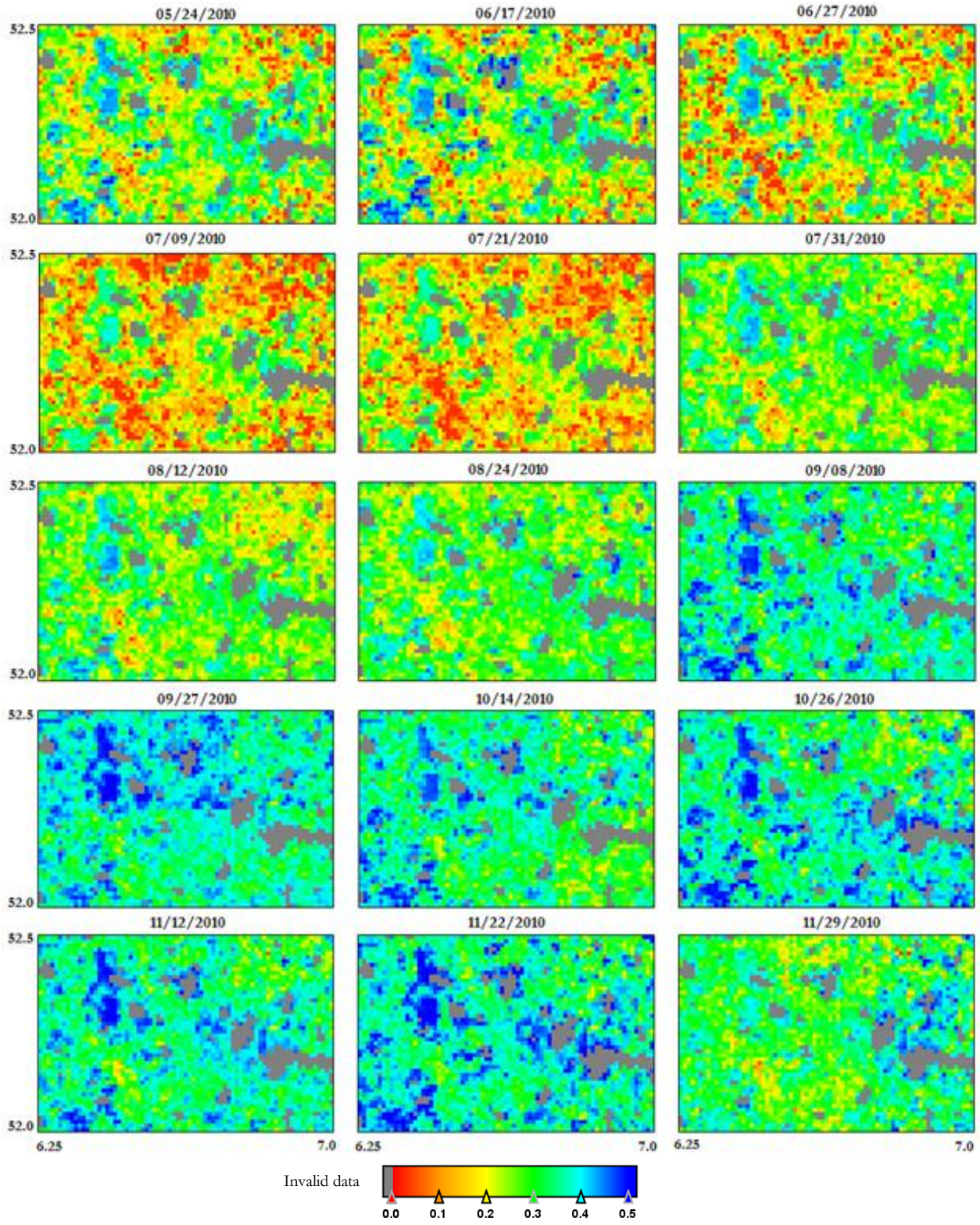

Figure 6.3- Series of soil moisture maps achieved by combining passive and active microwave observations over Twente region at 1-km resolution

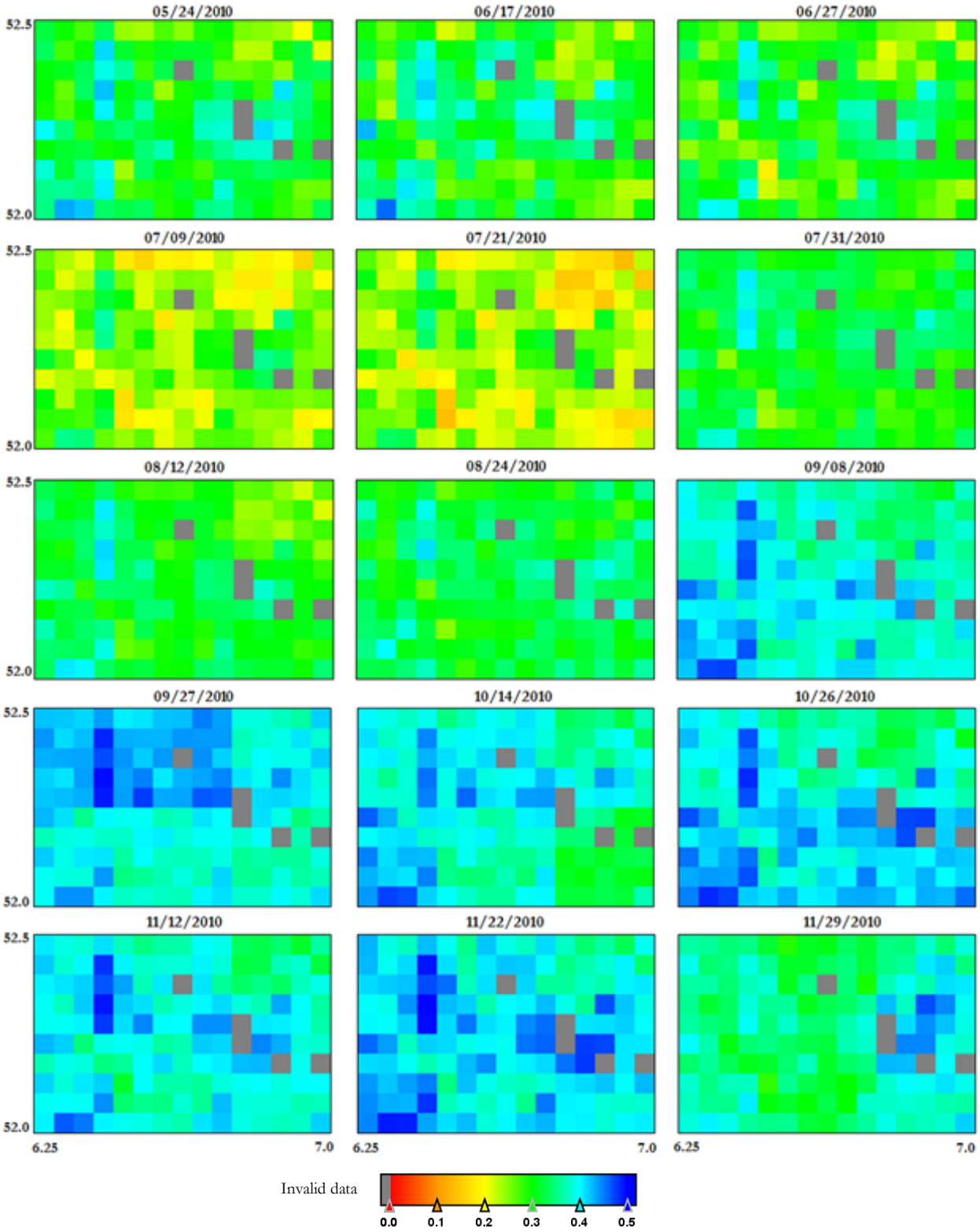

Figure 6.4- Series of soil moisture maps achieved by combining passive and active microwave observations over Twente region at 5-km resolution

7. CONCLUSIONS AND RECOMMENDATIONS

Conclusions

The main objective of this study was to retrieve validated soil moisture products at a medium spatial resolution (1-9 km) in a heterogeneous landscape by combining coarse resolution soil moisture products with high-resolution SAR observations. To retrieve soil moisture maps, the SMAP algorithm has been applied using the VUA-NASA soil moisture products and the PALSAR backscatter data sets over the Twente region. Validation was carried out by comparing the retrievals against in-situ measurements. Based on the obtained results from this comparison we conclude that:

- Application of the SMAP algorithm over a heterogeneous landscape results in higher resolution retrievals of soil moisture at reasonable accuracy satisfying the requirements for SAR-based soil moisture products (0.06 m^3 m^{-3}).

- Application of the SMAP algorithm improves the spatial representation of soil moisture within the radiometer footprint. This improvement demonstrates the potential of the algorithm for monitoring higher resolution soil moisture products with reasonable accuracy suitable for hydro-meteorological and agricultural related applications.

- A priori assumption on the homogeneity of the soil moisture sensitivity parameter (β) within the radiometer footprint increases the error of estimations by the SMAP algorithm over a heterogeneous landscape.

- Obtained soil moisture retrievals at coarser resolution (5-km) have better agreement with in-situ measurements. Because radar speckle noise has negative impact on the SMAP algorithm performance, this better compromise is attributed to the lower noise level in aggregated σ° to the coarser resolution.

- Even though the performance of the 5-km product is better than the 1-km product in terms of their accuracy, 1-km product provides better information on the temporal and spatial variability of soil moisture. For instance, the intensity and duration of the drought in 2010 is well reflected in the 1-km products, while the 5-km products could not capture it.

Recommendations

- The SMAP algorithm is developed to combine the L-band radar observations and L-band radiometric soil moisture products. For further assessment of the algorithm performance, consequently, we suggest applying the algorithm to the space-borne active/passive data sets at L-band.

- Application of the algorithm for soil moisture retrievals at coarser resolution than 5-km is also recommended to carry out evaluation of the algorithm performance in the presence of lower noise level.

LIST OF REFERENCES

Albertson, J. D., & Parlange, M. B. (1999). Natural integration of scalar fluxes from complex terrain. *Advances in Water Resources, 23*(3), 239-252.

Berg, A. A., Famiglietti, J. S., Walker, J. P., & Houser, P. R. (2003). Impact of bias correction to reanalysis products on simulations of North American soil moisture and hydrological fluxes. *Journal of Geophysical Research: Atmospheres, 108*(D16), n/a-n/a. doi: 10.1029/2002jd003334

Brocca, L., Hasenauer, S., Lacava, T., Melone, F., Moramarco, T., Wagner, W., . . . Bittelli, M. (2011). Soil moisture estimation through ASCAT and AMSR-E sensors: An intercomparison and validation study across Europe. *Remote Sensing of Environment, 115*(12), 3390-3408. doi: 10.1016/j.rse.2011.08.003

Calvet, J. C., Wigneron, J. P., Walker, J., Karbou, F., Chanzy, A., & Albergel, C. (2011). Sensitivity of Passive Microwave Observations to Soil Moisture and Vegetation Water Content: L-Band to W-Band. *Geoscience and Remote Sensing, IEEE Transactions on, 49*(4), 1190-1199. doi: 10.1109/tgrs.2010.2050488

Chauhan, N. S., Miller, S., & Ardanuy, P. (2003). Spaceborne soil moisture estimation at high resolution: a microwave-optical/IR synergistic approach. *International Journal of Remote Sensing, 24*(22), 4599-4622. doi: 10.1080/0143116031000156837

Das, N. N., Entekhabi, D., & Njoku, E. G. (2011). An Algorithm for Merging SMAP Radiometer and Radar Data for High-Resolution Soil-Moisture Retrieval. *Geoscience and Remote Sensing, IEEE Transactions on, 49*(5), 1504-1512. doi: 10.1109/tgrs.2010.2089526

Dente, L., Su, Z., & Wen, J. (2012). Validation of SMOS Soil Moisture Products over the Maqu and Twente Regions. *Sensors, 12*(8), 9965-9986.

Dobson, M. C., & Ulaby, F. T. (1986). Preliminaly Evaluation of the SIR-B Response to Soil Moisture, Surface Roughness, and Crop Canopy Cover. *Geoscience and Remote Sensing, IEEE Transactions on, GE-24*(4), 517-526. doi: 10.1109/tgrs.1986.289666

Dobson, M. C., Ulaby, F. T., LeToan, T., Beaudoin, A., Kasischke, E. S., & Christensen, N. (1992). Dependence of radar backscatter on coniferous forest biomass. *Geoscience and Remote Sensing, IEEE Transactions on, 30*(2), 412-415. doi: 10.1109/36.134090

Draper, C. S., Walker, J. P., Steinle, P. J., de Jeu, R. A. M., & Holmes, T. R. H. (2009). An evaluation of AMSR–E derived soil moisture over Australia. *Remote Sensing of Environment, 113*(4), 703-710. doi: http://dx.doi.org/10.1016/j.rse.2008.11.011

Entekhabi, D., Njoku, E., O'Neill, P., Spencer, M., Jackson, T., Entin, J., . . . Kellogg, K. (2008, 7-11 July 2008). *The Soil Moisture Active/Passive Mission (SMAP).* Paper presented at the Geoscience and Remote Sensing Symposium, 2008. IGARSS 2008. IEEE International.

Entekhabi, D., Njoku, E. G., O'Neill, P. E., Kellogg, K. H., Crow, W. T., Edelstein, W. N., . . . Johnson, J. (2010). The soil moisture active passive (SMAP) mission. *Proceedings of the IEEE, 98*(5), 704-716.

Ferrazzoli, P., & Guerriero, L. (1995). Radar sensitivity to tree geometry and woody volume: a model analysis. *Geoscience and Remote Sensing, IEEE Transactions on, 33*(2), 360-371. doi: 10.1109/36.377936

Gruhier, C., De Rosnay, P., Hasenauer, S., Holmes, T. R. H., De Jeu, R. A. M., Kerr, Y. H., . . . Wagner, W. (2010). Soil moisture active and passive microwave products: intercomparison and evaluation over a Sahelian site.

Hamazaki, T. (1999). *Overview of the Advanced Land Observing Satellite (ALOS): Its Mission Requirements, Sensors, and a Satellite System.* Paper presented at the ISPRS Joint Workshop "Sensors and Mapping from Space 1999", Hanover, Germany.

Huete, A., Didan, K., Miura, T., Rodriguez, E. P., Gao, X., & Ferreira, L. G. (2002). Overview of the radiometric and biophysical performance of the MODIS vegetation indices. *Remote Sensing of Environment, 83*(1), 195-213.

Ito, N., Hamazaki, T., & Tomioka, K. (2001). *ALOS/PALSAR characteristics and status.* Paper presented at the Proceedings of the CEOS SAR Workshop 2001.

Jackson, T. J. (1993). III. Measuring surface soil moisture using passive microwave remote sensing. *Hydrological processes, 7*(2), 139-152.

Jackson, T. J., Cosh, M. H., Bindlish, R., Starks, P. J., Bosch, D. D., Seyfried, M., . . . Jinyang, D. (2010). Validation of Advanced Microwave Scanning Radiometer Soil Moisture Products. *Geoscience and Remote Sensing, IEEE Transactions on, 48*(12), 4256-4272. doi: 10.1109/tgrs.2010.2051035

Joseph, A. T., van der Velde, R., O'Neill, P. E., Lang, R., & Gish, T. (2010). Effects of corn on C- and L-band radar backscatter: A correction method for soil moisture retrieval. *Remote Sensing of Environment, 114*(11), 2417-2430. doi: http://dx.doi.org/10.1016/j.rse.2010.05.017

Kim, Y., & van Zyl, J. J. (2009). A Time-Series Approach to Estimate Soil Moisture Using Polarimetric Radar Data. *Geoscience and Remote Sensing, IEEE Transactions on, 47*(8), 2519-2527. doi: 10.1109/tgrs.2009.2014944

Koike, T., Nakamura, Y., Kaihotsu, I., Davva, G., Matsuura, N., Tamagawa, K., & Fujii, H. (2004). Development of an Advanced Microwave Scanning Radiometer (AMSR-E) algorithm of soil moisture and vegetation water content. *Annual Journal of Hydraulic Engineering, JSCE, 48*(2), 217-222.

Koster, R. D., Guo, Z., Yang, R., Dirmeyer, P. A., Mitchell, K., & Puma, M. J. (2009). On the Nature of Soil Moisture in Land Surface Models. *Journal of Climate, 22*(16), 4322-4335. doi: 10.1175/2009jcli2832.1

Lievens, H., Verhoest, N., De Keyser, E., Vernieuwe, H., Matgen, P., Alvarez-Mozos, J., & De Baets, B. (2011). Effective roughness modelling as a tool for soil moisture retrieval from C-and L-band SAR. *Hydrology and Earth System Sciences, 15*(1), 151-162.

Löw, A., Ludwig, R., & Mauser, W. (2005). Use of microwave remote sensing data to monitor spatio temporal characteristics of surface soil moisture at local and regional scales. *Advances in Geosciences, 5*, 49-56.

Lu, H., Koike, T., Fujii, H., Ohta, T., & Tamagawa, K. (2009). Development of a physically-based soil moisture retrieval algorithm for spaceborne passive microwave radiometers and its application to AMSR-E. *Journal of The Remote Sensing Society of Japan, 29*.

Mattia, F., Satalino, G., & Balenzano, A. (2010). *Soil moisture retrieval from temporal series of PALSAR ScanSAR data.* Paper presented at the The 4th Joint PI Symposium of ALOS Data Nodes for ALOS Science Program, Tokyo, Japan.

Menges, C. H., van Zyl, J., Greg, G. J. E., & Ahmed, W. (2001). *Incidence angle correction of AirSAR data to facilitate land-cover classification* (Vol. 67). Bethesda, MD, ETATS-UNIS: American Society for Photogrammetry and Remote Sensing.

Merlin, O., Chehbouni, A., Kerr, Y. H., & Goodrich, D. C. (2006). A downscaling method for distributing surface soil moisture within a microwave pixel: Application to the Monsoon '90 data. *Remote Sensing of Environment, 101*(3), 379-389. doi: 10.1016/j.rse.2006.01.004

Merlin, O., Chehbouni, A. G., Kerr, Y. H., Njoku, E. G., & Entekhabi, D. (2005). A combined modeling and multispectral/multiresolution remote sensing approach for disaggregation of surface soil moisture: application to SMOS configuration. *Geoscience and Remote Sensing, IEEE Transactions on, 43*(9), 2036-2050. doi: 10.1109/tgrs.2005.853192

Merlin, O., Rudiger, C., Al Bitar, A., Richaume, P., Walker, J. P., & Kerr, Y. H. (2012). Disaggregation of SMOS Soil Moisture in Southeastern Australia. *Geoscience and Remote Sensing, IEEE Transactions on, 50*(5), 1556-1571. doi: 10.1109/tgrs.2011.2175000

Merlin, O., Walker, J. P., Chehbouni, A., & Kerr, Y. (2008). Towards deterministic downscaling of SMOS soil moisture using MODIS derived soil evaporative efficiency. *Remote Sensing of Environment, 112*(10), 3935-3946. doi: 10.1016/j.rse.2008.06.012

Miralles, D. G., Holmes, T. R. H., De Jeu, R. A. M., Gash, J. H., Meesters, A. G. C. A., & Dolman, A. J. (2011). Global land-surface evaporation estimated from satellite-based observations. *Hydrology and Earth System Sciences, 15*, 453-469.

Narayan, U., Lakshmi, V., & Jackson, T. J. (2006). High-resolution change estimation of soil moisture using L-band radiometer and Radar observations made during the SMEX02 experiments. *Geoscience and Remote Sensing, IEEE Transactions on, 44*(6), 1545-1554. doi: 10.1109/tgrs.2006.871199

Nicholson, S. E., Davenport, M. L., & Malo, A. R. (1990). A comparison of the vegetation response to rainfall in the Sahel and East Africa, using normalized difference vegetation index from NOAA AVHRR. *Climatic Change, 17*(2), 209-241.

Njoku, E. G., & Chan, S. K. (2006). Vegetation and surface roughness effects on AMSR-E land observations. *Remote Sensing of Environment, 100*(2), 190-199. doi: http://dx.doi.org/10.1016/j.rse.2005.10.017

Njoku, E. G., & Entekhabi, D. (1996). Passive microwave remote sensing of soil moisture. *Journal of Hydrology, 184*(1–2), 101-129. doi: 10.1016/0022-1694(95)02970-2

Njoku, E. G., Wilson, W. J., Yueh, S. H., Dinardo, S. J., Li, F. K., Jackson, T. J., . . . Bolten, J. (2002). Observations of soil moisture using a passive and active low-frequency microwave airborne sensor during SGP99. *Geoscience and Remote Sensing, IEEE Transactions on, 40*(12), 2659-2673. doi: 10.1109/tgrs.2002.807008

O'Neill, P. E., Chauhan, N. S., & Jackson, T. J. (1996). Use of active and passive microwave remote sensing for soil moisture estimation through corn. *International Journal of Remote Sensing, 17*(10), 1851-1865. doi: 10.1080/01431169608948743

Owe, M., de Jeu, R., & Holmes, T. (2008). Multisensor historical climatology of satellite-derived global land surface moisture. *J. Geophys. Res., 113*(F1), F01002. doi: 10.1029/2007jf000769

Owe, M., de Jeu, R., & Walker, J. (2001). A methodology for surface soil moisture and vegetation optical depth retrieval using the microwave polarization difference index. *Geoscience and Remote Sensing, IEEE Transactions on, 39*(8), 1643-1654. doi: 10.1109/36.942542

Piles, M., Camps, A., Vall-llossera, M., Corbella, I., Panciera, R., Rudiger, C., . . . Walker, J. (2011). Downscaling SMOS-Derived Soil Moisture Using MODIS Visible/Infrared Data. *Geoscience and Remote Sensing, IEEE Transactions on, 49*(9), 3156-3166. doi: 10.1109/tgrs.2011.2120615

Piles, M., Camps, A., Vall-llossera, M., Sanchez, N., Martinez-Fernandez, J., Monerris, A., . . . s, X. (2010, 1-4 March 2010). *Soil moisture downscaling activities at the REMEDHUS Cal/Val site and its application to SMOS*. Paper presented at the Microwave Radiometry and Remote Sensing of the Environment (MicroRad), 2010 11th Specialist Meeting on.

Piles, M., Entekhabi, D., & Camps, A. (2009). A Change Detection Algorithm for Retrieving High-Resolution Soil Moisture From SMAP Radar and Radiometer Observations. *Geoscience and Remote Sensing, IEEE Transactions on, 47*(12), 4125-4131. doi: 10.1109/tgrs.2009.2022088

Qiu, F., Berglund, J., Jensen, J. R., Thakkar, P., & Ren, D. (2004). Speckle Noise Reduction in SAR Imagery Using a Local Adaptive Median Filter. *GIScience & Remote Sensing, 41*(3). doi: 10.2747/1548-1603.41.3.244

Reichle, R. H. (2008). Data assimilation methods in the Earth sciences. *Advances in Water Resources, 31*(11), 1411-1418.

Rüdiger, C., Calvet, J. C., Gruhier, C., Holmes, T. R. H., de Jeu, R. A. M., & Wagner, W. (2009). An intercomparison of ERS-Scat and AMSR-E soil moisture observations with model simulations over France. *Journal of Hydrometeorology, 10*(2), 431-447.

Saatchi, S., Halligan, K., Despain, D. G., & Crabtree, R. L. (2007). Estimation of Forest Fuel Load From Radar Remote Sensing. *Geoscience and Remote Sensing, IEEE Transactions on, 45*(6), 1726-1740. doi: 10.1109/tgrs.2006.887002

Satalino, G., Mattia, F., Davidson, M. W. J., Thuy Le, T., Pasquariello, G., & Borgeaud, M. (2002). On current limits of soil moisture retrieval from ERS-SAR data. *Geoscience and Remote Sensing, IEEE Transactions on, 40*(11), 2438-2447. doi: 10.1109/tgrs.2002.803790

Schmugge, T. J., Kustas, W. P., Ritchie, J. C., Jackson, T. J., & Rango, A. (2002). Remote sensing in hydrology. *Advances in Water Resources, 25*(8–12), 1367-1385. doi: 10.1016/s0309-1708(02)00065-9

Schumann, G., Lunt, D. J., Valdes, P. J., de Jeu, R. A. M., Scipal, K., & Bates, P. D. (2009). Assessment of soil moisture fields from imperfect climate models with uncertain satellite observations. *Hydrology and Earth System Sciences, 13*, 1545-1553.

Shimada, M., Isoguchi, O., Tadono, T., & Isono, K. (2009). PALSAR radiometric and geometric calibration. *Geoscience and Remote Sensing, IEEE Transactions on, 47*(12), 3915-3932.

Shimada, M., Wakabayashi, H., Tadono, T., Rosenqvist, A., & Igarashi, T. (2001). Calibration and Validation of PALSAR and Research Products of NASDA/EORC. Retrieved from ftp://helios.eorc.jaxa.jp/cdroms/EORC-061/data/f_papers/ceos077.pdf

Su, Z., Wen, J., Dente, L., van der Velde, R., Wang, L., Ma, Y., . . . Hu, Z. (2011). The Tibetan Plateau observatory of plateau scale soil moisture and soil temperature (Tibet-Obs) for quantifying uncertainties in coarse resolution satellite and model products. *Hydrology and Earth System Sciences, 15*(7), 2303.

Thoma, D., Moran, M., Bryant, R., Rahman, M., Collins, C., Keefer, T., . . . Tischler, M. (2008). Appropriate scale of soil moisture retrieval from high resolution radar imagery for bare and minimally vegetated soils. *Remote Sensing of Environment, 112*(2), 403-414.

Ulaby, F. T., Moore, R. K., & Fung, A. K. (1982). *Microwave Remote Sensing Active and Passive* (Vol. II). Canada: Addison-Wesley Publishing Company.

Van der Velde, R., Salama, M. S., van Helvoirt, M. D., Su, Z., & Ma, Y. (2012b). Decomposition of Uncertainties between Coarse MM5–Noah-Simulated and Fine ASAR-Retrieved Soil Moisture over Central Tibet. *Journal of Hydrometeorology, 13*(6), 1925-1938. doi: 10.1175/jhm-d-11-0133.1

Van der Velde, R., & Su, Z. (2009). Dynamics in land-surface conditions on the Tibetan Plateau observed by Advanced Synthetic Aperture Radar (ASAR). *Hydrological Sciences Journal, 54*(6), 1079-1093. doi: 10.1623/hysj.54.6.1079

Van der Velde, R., Su, Z., & Ma, Y. (2008). Impact of Soil Moisture Dynamics on ASAR σo Signatures and Its Spatial Variability Observed over the Tibetan Plateau. *Sensors, 8*(9), 5479-5491.

Van der Velde, R., Su, Z., Van Oevelen, P., Wen, J., Ma, Y., & Salama, M. S. (2012a). Soil moisture mapping over the central part of the Tibetan Plateau using a series of ASAR WS images. *Remote Sensing of Environment, 120*(0), 175-187. doi: 10.1016/j.rse.2011.05.029

Van der Velde, R., Su, Z., & Van Oevelen, P. J. (2010). *Soil moisture remote sensing using active microwaves and land surface modeling.* (176), University of Twente Faculty of Geo-Information and Earth Observation ITC, Enschede. Retrieved from http://www.itc.nl/library/papers_2010/phd/vd_velde.pdf

Vinnikov, K. Y., Robock, A., Speraskaya, N. A., & Schlosser, C. A. (1996). Scales of temporal and spatial variability of midlatitude soil moisture. *Journal of Geophysical Research, 101*(D3), 7163-7174.

Wagner, W., Naeimi, V., Scipal, K., de Jeu, R., & Martínez-Fernández, J. (2007). Soil moisture from operational meteorological satellites. *Hydrogeology Journal, 15*(1), 121-131.

Wagner, W., Noll, J., Borgeaud, M., & Rott, H. (1999). Monitoring soil moisture over the Canadian Prairies with the ERS scatterometer. *Geoscience and Remote Sensing, IEEE Transactions on, 37*(1), 206-216. doi: 10.1109/36.739155

Wagner, W., Sabel, D., Doubkova, M., Bartsch, A., & Pathe, C. (2009). *The potential of Sentinel-1 for monitoring soil moisture with a high spatial resolution at global scale.* Paper presented at the Earth Observation and Water Cycle Science Symposium, Frascati, Italy.

Xia, Z.-G., & Sheng, Y. (1996, 27-31 May 1996). *Radar speckle: noise or information?* Paper presented at the Geoscience and Remote Sensing Symposium, 1996. IGARSS '96. 'Remote Sensing for a Sustainable Future.', International.

APPENDICES

Appendix 1- List of the utilized PALSAR data sets and their basic information

Index	Date	Central Overpass time	Orbit	Track	Orbital Acquisition
1	09/06/2008	10:27:00	12652	320	Descending
2	21/06/2008	10:22:42	12827	318	Descending
3	08/07/2008	10:24:56	13075	319	Descending
4	20/07/2008	10:20:40	13250	317	Descending
5	23/08/2008	10:25:33	13746	319	Descending
6	04/09/2008	10:21:30	13921	317	Descending
7	21/09/2008	10:23:58	14169	318	Descending
8	03/10/2008	10:19:55	14344	316	Descending
9	08/10/2008	10:26:27	14417	319	Descending
10	25/10/2008	10:28:54	14665	320	Descending
11	01/11/2008	10:18:18	14767	315	Descending
12	06/11/2008	10:24:50	14840	318	Descending
13	18/11/2008	10:20:44	15015	316	Descending
14	24/05/2010	10:22:40	23067	316	Descending
15	15/06/2010	10:31:02	23388	320	Descending
16	17/06/2010	10:13:50	23417	312	Descending
17	22/06/2010	10:20:14	23490	315	Descending
18	27/06/2010	10:26:37	23563	318	Descending
19	04/07/2010	10:15:48	23665	313	Descending
20	09/07/2010	10:22:12	23738	316	Descending
21	14/07/2010	10:28:35	23811	319	Descending
22	21/07/010	10:17:46	23913	314	Descending
23	26/07/2010	10:24:09	23986	317	Descending
24	31/07/2010	10:30:32	24059	320	Descending
25	02/08/2010	10:13:20	24088	312	Descending
26	07/08/2010	10:19:43	24161	315	Descending
27	12/08/2010	10:26:06	24234	318	Descending
28	19/08/2010	10:15:17	24336	313	Descending
29	24/08/2010	10:21:40	24409	316	Descending
30	29/08/2010	10:28:02	24482	319	Descending
31	08/09/2010	21:51:17	24635	647	Ascending
32	15/09/2010	10:29:58	24730	320	Descending
33	27/09/2010	10:25:29	24905	318	Descending
34	14/10/2010	10:27:23	25153	319	Descending
35	26/10/2010	10:22:54	25328	317	Descending
36	12/11/2010	10:24:48	25576	318	Descending
37	19/11/2010	10:13:56	25678	313	Descending
38	22/11/2010	21:47:59	25729	646	Ascending
39	24/11/2010	10:20:17	25751	316	Descending
40	29/11/2010	10:26:38	25824	319	Descending

Appendix 2- Statistical analysis of soil moisture retrievals from combination of LPRM soil moisture product and PALSAR σ°

	soil moisture retrievals at 1 km				**soil moisture retrievals at 5 km**			
Stations	**R^2**	**Bias**	**RMSE**	**MAE**	**R^2**	**Bias**	**RMSE**	**MAE**
ITCSM01	0.53	-0.108	0.133	0.116	0.62	-0.015	0.072	0.059
ITCSM02	0.28	0.215	0.228	0.215	0.56	0.164	0.172	0.164
ITCSM03	0.4	-0.111	0.128	0.114	0.53	-0.047	0.069	0.057
ITCSM04	0.37	0.207	0.219	0.207	0.52	0.134	0.149	0.134
ITCSM05	0.38	0.084	0.106	0.084	0.62	0.145	0.152	0.145
ITCSM06	0.45	0.092	0.123	0.103	0.6	0.102	0.116	0.105
ITCSM07	0.53	0.079	0.103	0.089	0.45	0.134	0.143	0.134
ITCSM08	0.57	0.147	0.156	0.147	0.28	0.217	0.226	0.217
ITCSM09	0.27	0.129	0.149	0.134	0.33	0.126	0.144	0.126
ITCSM10	0.48	-0.028	0.072	0.059	0.53	0.007	0.064	0.053
ITCSM11	0.11	0.121	0.148	0.128	0.34	0.086	0.11	0.086
ITCSM12	0.42	0.076	0.107	0.092	0.57	0.167	0.174	0.167
ITCSM13	0.32	0.084	0.106	0.087	0.13	0.188	0.201	0.188
ITCSM15	0.68	-0.015	0.053	0.037	0.53	0.025	0.061	0.043
ITCSM17	0.37	0.121	0.134	0.122	0.45	0.94	0.199	0.194
ITCSM18	0.43	0.103	0.122	0.104	0.32	0.157	0.172	0.157
ITCSM19	0.48	-0.036	0.086	0.066	0.69	0.054	0.082	0.069
ITCSM20	0.45	0.169	0.175	0.169	0.52	0.147	0.152	0.147

Appendix 3- Statistical analysis of soil moisture retrievals from combination of LPRM soil moisture products and PALSAR σ° after applying the bias correction on the retrievals

	Soil moisture at 1 km		**Soil moisture at 5 km**	
Stations	**RMSE**	**MAE**	**RMSE**	**MAE**
ITCSM01	0.076	0.062	0.069	0.06
ITCSM02	0.076	0.064	0.052	0.042
ITCSM03	0.064	0.05	0.05	0.038
ITCSM04	0.074	0.061	0.065	0.051
ITCSM05	0.065	0.049	0.047	0.036
ITCSM06	0.082	0.067	0.055	0.04
ITCSM07	0.066	0.053	0.049	0.038
ITCSM08	0.051	0.04	0.065	0.053
ITCSM09	0.075	0.062	0.068	0.06
ITCSM10	0.067	0.054	0.064	0.053
ITCSM11	0.086	0.067	0.071	0.058
ITCSM12	0.075	0.059	0.048	0.036
ITCSM13	0.065	0.053	0.071	0.06
ITCSM15	0.051	0.037	0.055	0.039
ITCSM17	0.056	0.045	0.049	0.04
ITCSM18	0.066	0.056	0.071	0.058
ITCSM19	0.078	0.056	0.061	0.048
ITCSM20	0.042	0.033	0.038	0.031

Appendix 4- Same as Table 5.1 (b) but after bias correction

Pixel	**RMSE**	**MAE**	**n**
(0,0)	0.055	0.043	3
(1,0)	0.047	0.036	4
(2,0)	0.042	0.032	5
(0,1)	0.063	0.051	1
(1,1)	0.044	0.031	4
(2,1)	0.067	0.059	1